Université d'Ottawa · University of Ottawa

Université d'Ottawa · University of Ottawa

FACULTÉ DES ÉTUDES SUPÉRIEURES ET POSTDOCTORALES

FACULTY OF GRADUATE AND POSTDOCTORAL STUDIES

OSTROVSKY, Marsha

AUTEUR DE LA THÈSE - AUTHOR OF THESIS

M.Sc. (Biology)

GRADE - DEGREE

Biology

FACULTÉ, ÉCOLE, DÉPARTEMENT - FACULTY, SCHOOL, DEPARTMENT

TITRE DE LA THÈSE - TITLE OF THE THESIS

Detecting Human Impacts on Ecosystem Function in Southern Canada

D. Currie

DIRECTEUR DE LA THÈSE - THESIS SUPERVISOR

EXAMINATEURS DE LA THÈSE - THESIS EXAMINERS

J.T. Arnason

N. Cappuccino

S. Findlay

J. Kerr

J.-M. De Koninck, Ph.D.

LE DOYEN DE LA FACULTÉ DES ÉTUDES SUPÉRIEURES ET POSTDOCTORALES

SIGNATURE

DEAN OF THE FACULTY OF GRADUATE AND POSTDOCTORAL STUDIES

Detecting Human Impacts on Ecosystem Function in Southern Canada

by

Marsha Ostrovsky

Thesis submitted to the Faculty of Graduate and Postdoctoral Studies, University of Ottawa,

in partial fulfillment of the requirements for the M.Sc. degree in the

Ottawa-Carleton Institute of Biology

Ottawa, Ontario, Canada

June 2003

Université d'Ottawa
University of Ottawa

Candidate

Supervisor

Your file Votre référence
ISBN: 0-612-90342-7
Our file Notre référence
ISBN: 0-612-90342-7

Acknowledgements

Whom better to thank at the beginning than my supervisor, David Currie. Without him, this project would have been nothing more than a random assemblage of numbers and letters. He imparted much ecological and culinary wisdom and gave me the opportunity to explore new terrain, at home and abroad, for which I am grateful. I greatly appreciate Jeremy Kerr's enthusiastic encouragement and much-needed remote sensing expertise and Scott Findlay's wit and boundless statistical knowledge. I thank Don Rivard at Parks Canada for believing in this project. I had the remarkable fortune of having both good friends and colleagues as lab mates: Tania Sendel, Tony Francis, Joëlle Pinsonnault, Line Pepin, Dagoberto Hernandez, Attila Kalmar, and Bryan Wilson made long days at the computer infinitely more bearable. Thank you to Robin Mackey, who was always up for a session of skating and commiserating. Thanks also to the great people in the Findlay, Morin, and Pick labs for Friday afternoon beer dates and for listening. Veronica Diaz, Jessica Head, Katrine Ireland, Sandra Luz, and Candace Webb are amazing friends who were always there. My family and friends in Toronto never lost faith in me. A huge thank you to my older brother, Dennis, for giving me peace of mind and support through a steady stream of e-mails and phone calls, and my younger brother, Martin, who said, "dooo iiiiiiit!". Dr. Dan McKenney of the Canadian Forest Service kindly provided me with climate data. I am grateful to NSERC, OGS, and Parks Canada for project funding and rent money.

Last, I have to thank two people who supported me unconditionally, worried about me incessantly, and sacrificed so much so that I could be here today: mom and dad, I dedicate this to you.

Table of Contents

Abstract

Human activities potentially threaten key ecological processes, or "ecosystem functions", mainly through the habitat conversion associated with urbanization and agriculture. Although ecosystem functions can clearly be disrupted in severely degraded systems, it is not clear how those functions vary along the entire gradient of human activity at scales most relevant to global environmental change. To address this question, I used two remotely sensed indices of ecosystem function, as measured by the normalized difference vegetation index (NDVI) and thermal infrared radiation (TIR), to derive estimates of primary productivity and evapotranspiration, respectively, at 1-km resolution across multiple vegetation types in southern Canada. After controlling for the variation in NDVI and TIR related to the climatic gradient, I related these indices to measures of anthropogenic activity (road density, extent of natural cover, and protected areas status). While NDVI and TIR are both strongly related to climate and vegetation type, much of the residual variation in NDVI (up to 67%) and TIR (up to 55%) is related to human activity. Ecosystems in areas of intense human impact are generally less productive and exhibit less water cycling (i.e., energy-transforming) efficiency, but I found no evidence of threshold effects in the response of ecosystem function to increasing human impact. Ecosystems in protected areas (parks and reserves) have significantly higher productivity and , to a lesser extent, higher evapotranspiration, which suggests increased solar energy-transforming capacity. These relationships are strongest at coarse spatial scales and are generally consistent within different vegetation types. The magnitude of these effects along the entire gradient of human activity is substantial.

Résumé

En général, la transformation des habitats naturels causée par les activités humaines, notamment l'urbanisation et l'agriculture, peuvent menacer des processus écologiques clés, ou les fonctions de l'écosystème. Parmi ces fonctions sont la purification de l'air et l'eau, la circulation des nutriments et le maintien de la fertilité du sol. Bien que les fonctions de l'écosystème puissent être nettement perturbées dans des systèmes gravement détériorés, il n'est pas clair comment celles-ci varient le long du gradient d'activités humaines aux échelles les plus pertinentes par rapport aux changements environnementaux globaux.Afin d'aborder ce problème, j'ai utilisé deux indices par télédétection des fonctions de l'écosystème, soit l'indice d'activité végétale (IAV) et le spectre de l'infrarouge thermique (SIT), ce qui me permet d'établir des estimations de production primaire et d'évapotranspiration, respectivement, avec une résolution d'un kilomètre pour de multiples types de végétation dans le sud du Canada. Après avoir contrôlé les parties de la variance de l'IAV et du SIT qui sont associées aux gradients climatiques, j'ai établi un lien entre ces indices et les mesures d'activité anthropogénique (densité routière et étendue du couvert naturel) et la part d'aire protégée. Alors que l'IAV et le SIT sont tous deux fortement associés au climat et au type de végétation, la variance résiduelle de l'IAV (jusqu'à 67%) et du SIT (jusqu'à 55%) est en grande partie attribuable à l'activité humaine. Les écosystèmes se trouvant dans les zones fortement influencées par les facteurs anthropogéniques sont généralement moins productifs et l'évaporation de l'eau (la dégradation d'énergie) est moins efficace. Pourtant, je n'ai trouvé aucune évidence qu'il existe une seuil critique d'activité humaine au-delà de laquelle le fonctionnement écologique détériore rapidement. En outre, les écosystèmes dans des aires protégés (parcs) sont plus productifs et qui, dans une moindre

mesure, évaporent plus d'eau, ce qui laisse entendre que la capacité de dégradation d'énergie solaire est réduite. Ces relations sont plus significatives à une plus large échelle spatiale et sont généralement constantes pour les divers types de végétations. L'ampleur de ces effets le long du gradient d'activités humaines est considérable.

List of Tables

protected area status) and climate and vegetation type. All models are of the following form: anthropogenic variable = $(\text{precipitation})^{0.2}$ + temperature + $(\text{precipitation})^{0.2}$*temperature + vegetation + constant, where *vegetation* represents a categorical variable consisting of 10 land use classes.

Table 6. Summary of general linear model results ($r^2 \pm 95\%$ C. I.) examining the dependence of NDVI (normalized difference vegetation index) and of TIR (thermal infrared radiation) on natural environmental factors (temperature, precipitation, vegetation type) versus anthropogenic variables (road density, extent of natural cover, and park area) across spatial scales, where *n* represents sample size averaged over four replicates and *p* represents the significance of the aggregate variation explained by human activity (road density, natural cover) and park area in the total model (natural + human). *Human only* r^2 indicates the variation in NDVI and TIR related to road density, extent of natural cover, and park area *before* controlling for climate and vegetation type. Park area, which is added last in the models, remains statistically significant at all spatial scales ($p<0.05$).

Table 7. Summary of general linear model results ($r^2 \pm 95\%$ C. I.) examining the dependence of NDVI (normalized difference vegetation index) and of TIR (thermal infrared radiation) on $(\text{road density})^{0.2}$, natural cover, and $(\text{park area})^{0.2}$ across spatial scales, where *vegetation* is a 10-class categorical variable and *p* represents the significance of the variation explained by each of the anthropogenic variables in the following model: $(\text{precipitation})^{0.2}$ + temperature + $(\text{precipitation})^{0.2}$*temperature + vegetation + (road density *or* natural cover *or* park area)*vegetation.

Table 8. Sample results from an analysis of covariance examining the dependence of NDVI (normalized difference vegetation index) and of TIR (thermal infrared radiation) on natural characteristics of the environment—temperature, precipitation ($precipitation^{0.2}$), and vegetation (10-class categorical variable)—and anthropogenic variables—road density, extent of natural cover, and park area—for a quadrat size of 18825 km^2. Human activity variables entered singly in these models were never significant. Collinearity among climate and anthropogenic variables occasionally resulted in non-significant p-values for model terms.

Table 9. Summary of linear regressions (pooled over replicates at each quadrat size) examining the direction of the vegetation-specific responses of NDVI (normalized difference vegetation index) and TIR (thermal infrared radiation) to human activity – road density and extent of natural cover – and protected area status (park area). Results are based on a 10-class vegetation classification. Numerical values indicate how frequently a significant relationship ($p<0.05$) is observed across spatial scales (out of five quadrat sizes) and direction of relationships is indicated by a (+) or (–) sign. Vegetation types are described in more detail in Table 1.

Figure Legends

Figure 1. Land use map of Canada derived from 1998 SPOT-4/VGT imagery.

Figure 2. Seasonally-averaged normalized difference vegetation index (NDVI) in Canada (1994-2000) for a quadrat size of 675 km^2. NDVI is derived from the visible and near infrared channels of the NOAA-AVHRR sensor.

Figure 3. Seasonally-integrated thermal infrared radiation (TIR) in Canada (1994-2000) for a quadrat size of 675 km^2. TIR is derived from thermal channels 4 and 5 of the NOAA-AVHRR sensor. Sites where TIR is visibly higher than the surrounding landscape include the Okanagan Valley of British Columbia (1); small patches of agriculture in areas of boreal forest north of Lake Huron (2), southern Ontario and the Eastern Townships of Québec (3); and the James Bay-LaGrande hydroelectric project (4).

Figure 4. Total growing season precipitation (April to October) normalized for the years 1961-1990 for a quadrat size of 675 km^2.

Figure 5. Mean growing season temperature (April to October) normalized for the years 1961 to 1990 for a quadrat size of 675 km^2.

Figure 6. Road density in Canada for a quadrat size of 675 km^2.

Figure 7. Protected area status in Canada for a quadrat size of 676 km^2. Protected areas include all national, provincial, and municipal parks and conservation areas.

Figure 8. Normalized difference vegetation index (NDVI) and thermal infrared radiation (TIR) plotted as a function of human activity (road density, extent of natural cover) and protected area status before controlling for climate and vegetation type, shown for a quadrat size of 18225 km^2. NDVI- and TIR-road density curves are fitted with

two separate lines for two different groups of vegetation types: (i) pasture, low density pasture, woodland-agriculture, pasture/forest/cropland, and forest classes (○) and (ii) grassland/pasture, rangeland, and grain/canola (×).

Figure 9. Normalized difference vegetation index (NDVI) and thermal infrared radiation (TIR) residuals plotted as a function of human activity (road density, extent of natural cover) and protected area status residuals, after controlling for the variation related to climate and vegetation type in both the dependent and independent variables. Relationships are fitted with a Lowess curve and significance is based on linear regressions using data from all four replicates at a quadrat size of 18225 km^2, where each symbol represents a different replicate. All slopes are statistically significant ($p<0.05$).

Figure 10. Above expected and below expected ecosystem function as measured by seasonally-averaged NDVI (normalized difference vegetation index) for a quadrat size of 675 km^2, expressed in units of standard deviation (s.d.). Orange and yellow areas represent ecosystems in which observed NDVI is lower than expected, while green regions are those ecosystems in which NDVI is greater than expected. Grey regions are within one standard deviation of the expected NDVI. Excluded data represent areas with road density less than 0.001 km/km^2.

Figure 11. Schematic diagram showing the extent to which anthropogenic variables (road density, natural cover, and protected area status) covary with the natural environmental gradient, based on the results of general linear models (Table 6). The size of each bar (drawn to scale) shows the proportion of variation in NDVI (normalized difference vegetation index) statistically explained by the total model

(natural + human), natural only, human only, and natural or human. Variance was partitioned by examining the amounts of variance statistically explained when variables were added sequentially into regression models.

Introduction

Humans exert a great influence on the earth's ecological processes, often to the detriment of other species and the human enterprise itself (Balmford et al. 2002; Wackernagel et al. 2002). Human appropriation of a large portion of the earth's net primary productivity through urbanization and expanding agriculture (Vitousek et al. 1986, Wright 1990, Krausmann 2001), and conversion of natural habitats to other uses, threatens key ecological processes or "ecosystem functions" in a habitat-specific way (Seabloom et al. 2002). These functions include air and water purification, nutrient cycling, crop pollination, and maintenance of soil fertility (Daily 1997, Kremen et al. 2002). Loss of diversity through habitat degradation – including species, genetic, and landscape diversity – is also believed to compromise ecosystem function (Ehrlich and Ehrlich 1981, Smith et al. 1995), although strong empirical evidence is generally lacking (Huston 1997, Loreau et al. 2001, Naeem 2002). The current human economy, which so strongly depends upon exploitation of the earth through deforestation and intensive agriculture, may ultimately undermine the processes that make life on earth possible.

Ecosystems tend to respond to human-induced perturbations in similar ways (Rapport et al. 1998). Most scientific understanding of ecosystem processes has been gained by direct field measurements and experiments on small study plots usually smaller than 1 ha (Waring and Running 1998). Whole-watershed studies like those conducted at the Hubbard Brook Experimental Forest are rare but have shown that deforestation, for example, leads to increased nutrient loss, reduced water cycling, reduced energy flows, reduced productivity, and reduced soil fertility (Bormann and Likens 1994). In deforested watersheds, streamflow is much higher because evapotranspiration is limited only to evaporation from the soil surface, while nitrogen and potassium, which are used in large quantities by plants, show the greatest increase in loss rates (Bormann and Likens 1994; Perakis and Hedin 2002). However, since most studies of human impact on ecosystem function are of severely degraded ecosystems at local spatial scales, little empirical knowledge exists on the relationship between ecosystem function and human activity across ecosystem types at landscape or regional scales (Paruelo et al. 2001).

Perceived human impacts on ecosystem function will depend greatly on the scale of observation. First, biological processes depend on different abiotic factors at different spatial scales (Levin 1992). For example, at local spatial scales (e.g., watersheds), spatial variation in net primary productivity depends on vegetation type, edaphic factors (e.g., parent material, nutrient concentration, soil moisture and texture), slope, and aspect. Over a global geographic extent, among-site differences in net primary productivity are mainly related to seasonal patterns of precipitation and temperature (Rosenzweig 1968; Leith 1975). Second, human activities can also influence ecosystem functions at multiple spatial scales (Gibson et al. 2000) – from individual forest stands to entire watersheds and landscapes. Due to the complex relationship between ecosystem processes, abiotic factors, and human activity, relationships between ecosystem function and human activity may be most obvious at certain scales (Kok and Veldekamp 2001).

Recently, remote sensing has been used to assess impacts of human activity on key ecosystem functions at landscape and regional scales, which are the scales most relevant to major ecological concerns (Waring and Running 1998; DeFries 2002). While no single agreed-upon metric exists to quantify ecosystem functioning (Goldstein 1999), processes such as primary productivity and water cycling (or evapotranspiration) are thought to be essential to "ecological integrity" (Schläpfer et al. 1999, Costanza 1999). Primary productivity and evapotranspiration can be remotely estimated using the normalized difference vegetation index (NDVI) and thermal infrared radiation (TIR), respectively. Strong theoretical and empirical evidence supports a near-linear relationship between NDVI and the fraction of photosynthetically active radiation (PAR) absorbed by the canopy, which in turn is strongly related to the productivity of ecosystems (Sellers 1985; Goward et al. 1985; Running and Nemani 1988; Box et al. 1989; Cihlar et al. 1991; Sellers et al. 1992). While this relationship becomes non-linear at saturating levels of PAR, vegetation indices are capable of indicating area-averaged rates of vegetation processes (i.e., photosynthesis, transpiration) (Sellers et al. 1992).

At local and regional scales, TIR reflects the "energy-transforming ability" of an ecosystem (Schneider and Kay 1994; Roy 1997; Quattrochi and Luvall 1999, which depends strongly on evapotranspiration.. Terrestrial ecosystems grow and develop by transforming the energetic gradient imposed on them by the sun (Schneider and Kay 1994). Most of the solar radiation absorbed by plants is converted to the latent heat of evaporation of water from the canopy (Budykov 1974; Waring and Running 1998). As well as driving many physiological processes in plants, evapotranspiration reduces the amount of energy re-radiated as heat, thus leading to lower re-radiated temperatures (TIR). As ecosystems mature, they develop more closed cycles and more water is evaporated from the canopy as opposed to being lost via run-off. Consequently, because ecosystems with greater functional and structural complexity evaporate more water, TIR is lower in more complex ecosystems (i.e., they will have lower re-radiated temperatures, Schneider and Kay 1994) and it increases as ecosystem diversity is reduced (Luvall and Holbo 1991). This trend in TIR has been found using airborne monitoring of mature Douglas fir forests (mature, complex) and recently regenerated clearcuts (simple, less complex) (Quattrochi and Luvall 1999). TIR has also been useful in the detection of weeds (i.e., increased diversity) in agricultural fields (Kay et al. 2002). Thus, a simplified or disturbed ecosystem will evaporate water less efficienty, leading to greater surface run-off and consequently, increased nutrient loss (Schneider and Kay 1994; Bormann and Likens 1994).

Although ecosystem function can clearly be disrupted in severely degraded systems, it is not clear how those functions vary along the entire gradient of human activity, nor whether current levels of human activity have led to widespread declines in function. My objective was to determine whether, across southern Canada, ecosystem function as measured by NDVI and TIR varies systematically with the intensity of human activity, which ranges from undetectably small to severe. Across broad geographic extents, a good proxy of human activity is the presence of roads. Roads can negatively influence ecosystems directly (Forman 2000, Trombulak and Frissell 2000), but more importantly, many types of human activities that accompany roads, such as urbanization, mining, agriculture, industrial activities, and logging are considered major threats to ecosystem function (Czech et al. 2000).

I hypothesized that ecosystem function is a function of certain natural environmental variables (viz. climate and vegetation type), proxies of human activity (road density, human-dominated land cover), and protected area status. Habitat destruction, and the resulting loss of biodiversity, is also thought to reduce ecosystem function; it can be approximated by measuring the extent of natural cover (non-agricultural and non-urban areas). Finally, I examined the relationship between ecosystem function and protected area status. In Canada, protection of ecological integrity has become central to the mandate of Parks Canada (Parks Canada Agency 2000). Maintenance of ecological processes is considered essential to achieving this goal. Therefore, I also determined whether protected area status, that is, how much of an area is occupied by national, provincial, or municipal parks and conservation areas, is related to ecosystem function. I evaluated the direction of the relationship between my two indices of ecosystem function, NDVI and TIR, and all three anthropogenic variables, both across and within vegetation types. I also asked if these relationships depend upon the grain of the analysis because of the variability in the scale of influence of both natural environmental factors and human activities.

Methods

Data Sources

I used biweekly, seasonally-averaged NDVI and seasonally-integrated TIR composites for April to October representing the years 1994 through 2000, provided by the Canada Centre for Remote Sensing (CCRS) in Ottawa, ON, Canada. Pixel size was 1 km^2. TIR was computed from the reflectance in channel 4 (thermal infrared, 1030-1140 nm) and channel 5 (thermal infrared, 1140-1240 nm) from the AVHRR sensor aboard the NOAA-11 and -14 satellites. The algorithm used to derive TIR from the thermal infrared channels is described in detail by Latifovic (2002). NDVI was computed from the intensity of reflected radiation in channel 1 (red, 580-680 nm) and channel 2 (near infrared, 725-1100 nm) from the AVHRR sensor aboard the NOAA-14 satellite:

NDVI = (Channel 1 – Channel 2)/(Channel 1 + Channel2)

Images were corrected by CCRS for atmospheric attenuation using the bi-directional reflectance function and were geometrically registered to the Lambert Conformal Conic map projection. The TIR images were also adjusted to account for differing surface emissivities. Further details on atmospheric correction, scene selection, radiometric calibration, and scene compositing can be found in Cihlar et al. (2002).

I obtained precipitation and temperature grids for the years 1961 to 1990, from the Canadian Forest Service. McKenney et al. (2001) used the thin plate spline technique to interpolate irregularly spaced climate station data, producing 300 arc second-resolution grids depicting mean monthly temperature and total monthly precipitation for all of Canada. I calculated mean annual temperature and total annual precipitation by averaging these monthly climate grids in Arc/Info®.

To control for the variation in NDVI and TIR related to vegetation type, I modified Kerr and Cihlar's (2003) original 25-class land use map based on a 1-km^2 resolution 1998 SPOT 4/Vegetation image (Cihlar et al. 2002). Within each land use class, I examined the ranges of, and correlations between, the ecosystem function and climate variables. I then grouped land use classes in which ecosystem function-climate relationships were statistically indistinguishable, reducing the number of classes from 25 to 10 (Fig. 1). I performed subsequent statistical analyses using this 10-class vegetation classification (Table 1).

To calculate road density, I used vector format CanMap® streetfiles, which cover most urban and rural areas in Canada (as of the 1996 Census) (DMTI Spatial Inc. 2001). The streetfiles were derived from the National Topographic Data Base and mapped at a scale of 1:250 000, which corresponds to a resolution of 125 m. The existing road classification assigned impact ratings to roads based on surface type, which varied from a value of 1 for unpaved two-lane roads to a value of 6 for four-lane expressways/highways (the largest road size in the database). I reassigned the impact ratings to create the following classifications to determine which transformation method allowed the best detection of human impact: (i) all roads received an equal weighting of one, (ii) roads received an impact rating approximately proportional to their area, or (iii) roads received an impact rating according to a geometric series ($2^{class-1}$, using the original 6 class system), with final values ranging from 1 to 32, to increase the difference among road types. To prepare each road density map, I first multiplied the length of each road by its impact rating. Using Arc/Info®, I then found the weighted line density per 1 km^2, resulting in a 1-km^2 resolution grid of road density. In all statistical models, only the third road classification was statistically significant, likely because larger roads are better associated with human activities.

I calculated protected area status as the proportion of a given sample area occupied by parks (abbreviated to "park area" in model equations, tables, and figures) using a vector file representing most protected areas in Canada, including national and provincial parks, park reserves, and conservation areas (unpublished data, World Wildlife Fund).

I used Arc/Info® to extract the data from my digital maps using a randomly placed sampling grid consisting of equal-area quadrats (225 km^2). Because the scale of analysis can greatly influence the identification of ecosystem function-human activity relationships, I tested whether my results depend upon spatial scale. I constructed similar grids with quadrat areas of 675, 2025, 6075, and 18225 km^2. Quadrat sizes were selected on the basis of their relevance to land use planning and the hierarchical organization of political jurisdictions: small quadrats correspond roughly to the size of townships and counties, while the large quadrats are similar in size to smaller provinces. Quadrats having more than 75% of their area covered by water, and/or falling outside the boundaries of Canada, were excluded.

To estimate the error associated with arbitrary placement of the sampling grid, I randomly relocated each grid and re-extracted the data from the digital maps, creating a total of four replicate data sets for each quadrat size. Random relocation of the sampling grid resulted in different numbers of quadrats being excluded from each replicate data set, depending on where quadrats fell with respect to borders or shorelines. Hence, sample size varied slightly among replicate data sets. However, when quadrat size was included as a covariate in statistical models, it was generally non-significant.

Since I was testing relationships between ecosystem function and human activity, I restricted my analysis only to those areas with detectable levels of human activity: quadrats located below 60° N and containing a road density greater than 0.001 km/km^2. While presence of roads is strongly associated with many types of human activity, the distribution of logging roads was not available in my road database. Hence road densities may underestimate forestry and mining activities, which are not explicitly identified in land use maps. I also masked out major urban areas because interpretation of remotely sensed characteristics of urban pixels is often problematic, and because this study is not designed to address human impacts in urban areas. Areas classified as urban are those census subdivisions with a population of at least 1,000 and an overall population density of at least 400 per km^2 (Statistics Canada 2001). For example, this definition led me to mask an area of 1286 km^2 in Toronto and an area of 1020 km^2 in Calgary. I assigned quadrats to a particular vegetation type according to the most dominant vegetation type present. To calculate the extent of natural cover in each quadrat, I calculated the total area of all vegetation types except those classified as agricultural.

Statistical Methodologies

I first examined variable distributions and collinearities. I tested normality of the data using a Kolmogorov-Smirnov test (Zar 1999) and applied the following transformations to yield approximately symmetrical distributions: $(\text{precipitation})^{0.2}$, $(\text{road density})^{0.2}$, and $(\text{park area})^{0.2}$. I then determined how spatial scale influenced the among-quadrat mean, range, and standard deviation of each variable (Table 2). Ecosystem function and anthropogenic variable statistics for each vegetation type are presented in Appendix A. To determine the degree of collinearity among my independent variables, I calculated Spearman rank correlations (Table 3).

Before testing for relationships with human activities and protected area status, I examined the results of general linear models to determine how much of the variation in NDVI and TIR can be related to patterns of precipitation and temperature in Canada. In the models, protected area status is referred to as an "anthropogenic variable", but not a human activity per se, because its influence on ecosystem function is expected to be different from that of increasing urbanization and agriculture, whose effects are expected to be negative. I selected the statistically simplest models that had homoscedastic residuals.

A one-way analysis of variance showed that NDVI and TIR differ significantly among different vegetation types. Therefore, to determine whether NDVI and TIR are significantly related to both climate and vegetation type, I used the following analysis of covariance:

$$\begin{aligned} \text{dependent variable} = {} & (\text{precipitation})^{0.2} \\ & + \text{temperature} \\ & + (\text{precipitation})^{0.2} * \text{temperature} \\ & + \text{VEGETATION} \\ & + \text{residual variance} \end{aligned} \tag{1}$$

where the dependent variables were NDVI and TIR, and where VEGETATION was the categorical vegetation type variable consisting of 10 classes.

Since humans have settled and established numerous smaller parks primarily in the southern part of Canada (less numerous but larger parks in the north), I tested how strongly these anthropogenic variables covary with the natural environmental gradient using model (1), where the dependent variable became road density, natural cover, or protected area status.

To test whether anthropogenic variables explain a significant amount of variation in NDVI and TIR *before* controlling for the natural environmental gradient, I examined the results of the following general linear models:

$$\begin{aligned}\text{dependent variable} = \ & (\text{road density})^{0.2} \\ & + \text{natural cover} \\ & + (\text{park area})^{0.2} \\ & + \text{residual variance}\end{aligned} \tag{2}$$

where the dependent variables were NDVI and TIR. The results of these models set the upper limit for the potential amount of variation in NDVI and TIR attributable to my measures of anthropogenic activity.

To test whether anthropogenic variables on aggregate explain a significant amount of variation in NDVI and TIR *after* controlling for the natural environmental gradient, I examined the results of the following general linear models:

$$\begin{aligned}\text{dependent variable} = \ & (\text{precipitation})^{0.2} \\ & + \text{temperature} \\ & + (\text{precipitation})^{0.2} * \text{temperature} \\ & + \text{VEGETATION} \\ & + \text{VEGETATION} * (\text{road density})^{0.2} \\ & + \text{VEGETATION} * \text{natural cover} \\ & + \text{VEGETATION} * (\text{park area})^{0.2} \\ & + \text{residual variance}\end{aligned} \tag{3}$$

where the dependent variables were NDVI and TIR. First-order anthropogenic terms were not included in model (3) because both first-order terms and interaction terms became non-significant. I found that the best model fit included interaction terms only. To determine if protected area status was significant after controlling for road density and natural cover, I added park area last in the model. I calculated the F statistic for anthropogenic factors on aggregate (road density, extent of natural cover, and amount of park area) as the ratio of (a) the difference in mean square between the model with climate and vegetation type only (1) and the model including all anthropogenic variables (3) and (b) the residual mean square from model (3). I considered the significance of human activities both independently and in conjunction with protected area status.

To determine how much of the residual variation in NDVI and TIR was related to individual measures of human activity, I used the following model:

$$\begin{aligned}\text{dependent variable} = {} & (\text{precipitation})^{0.2} \\ & + \text{temperature} \\ & + (\text{precipitation})^{0.2} * \text{temperature} \\ & + \text{VEGETATION} \\ & + \text{VEGETATION} * \text{human activity} \\ & + \text{residual variance}\end{aligned} \tag{4}$$

where the dependent variables were NDVI and TIR and the human activity variables were $(\text{road density})^{0.2}$ or natural cover. As before, I calculated the F statistic to test the significance of each human activity variable in the model. I repeated this process for protected area status, i.e. $(\text{park area})^{0.2}$.

I also calculated Moran's I to find the amount of spatial autocorrelation in model (3) residuals at each quadrat size. I determined the minimum number of independent samples required at each spatial scale for the relationships to remain statistically significant.

In addition, because it is possible that measurement error in the dependent variables changes with scale, I estimated measurement error for NDVI and TIR by calculating the interannual variation for ten randomly selected three-year averages. I repeated this procedure for a single replicate data set at each spatial scale.

To find the overall slope of the ecosystem function-human activity relationships, I used the residuals from models identical to (1), with NDVI and TIR as the dependent variables, with the exception that I ran the models by vegetation type (i.e., no categorical variable). I ran model (1) with human activity variables (road density and natural cover) and protected area status (park area) as the dependent variables to generate a second set of residuals. I then pooled data from all four replicate data sets at each quadrat size and used the following linear regressions to determine the slopes of the relationships at each spatial scale:

$$\text{dependent variable} = \text{human activity} \\ + \text{residual variance} \tag{5}$$

where the dependent variables were NDVI residuals and TIR residuals and the human activity variables were residuals of road density, natural cover, or protected area status. I determined the degree of correlation between NDVI and TIR within the 10 vegetation types by calculating Pearson correlation coefficients. For each vegetation type, I pooled the data over all replicate data sets at each spatial scale.

To determine the direction of the ecosystem function-human activity relationships within vegetation types, I examined the results of model (5) by pooling data over replicates within vegetation types at each spatial scale and recorded how many of the relationships were significant, as well as their sign, out of a possible total of five (i.e., five quadrat sizes).

I repeated this procedure to determine the direction of the relationship between ecosystem function and protected area status. To obtain an approximate measure of the observed change in net primary productivity across the range of road density, I used Figure 5 in Goward et al. (1985) showing the relationship between biome-averaged seasonally integrated NDVI (based on 90 measurements) and published values of mean biome net primary productivity.

Finally, to illustrate the spatial variability in ecosystem function across southern Canada, I created a map of "above expected" and "below expected" NDVI displaying the extent to which observed NDVI deviates from expected values. I used the residuals from model (1) to control for the variation in NDVI related to climate and vegetation type and calculated the mean and standard deviation of those residuals. I then classified ecosystem function across Canada based on the degree of deviation of observed NDVI from expected values.

In all my statistical models, p-values <0.05 were considered to be statistically significant.

Results

Prior to considering the relationships between human activity and my two measures of ecosystem function—the normalized difference vegetation index (NDVI) and thermal infrared radiation (TIR)—I examined their variation along natural environmental gradients, as well as the collinearities between human and natural variables.

Natural Variation in NDVI and TIR

In Canada, much of the broad-scale variation in NDVI (Fig. 2) and TIR (Fig. 3) is related to climate and vegetation type. Temperature and precipitation alone statistically explain from 69% to 78% of the variation in NDVI and from 84% to 91% of the variation in TIR, depending on the spatial scale (i.e., quadrats ranging from 225 km^2 to 18225 km^2) (Table 4). NDVI and TIR are not only strongly related to climate, they also differ significantly among vegetation types (ANOVA, $F>47$, $p<10^{-4}$). Although vegetation type and climate are collinear in Canada (Fig.4, Fig. 5), NDVI and TIR depend significantly upon both sets of variables, even after controlling for the variation attributable to one or the other (ANCOVA, $p<10^{-4}$). Combined, climate and vegetation type explain 83% to 89% of the variation in NDVI and 90% to 94% of the variation in TIR (Table 4).

Anthropogenic Activity and the Natural Environmental Gradient

Human activity, as measured by road density (Fig. 6), is highest in the southern half of Canada where climate is most favourable. Regions of higher road density are associated with extensive agriculture and urbanization in the south, and to a lesser degree with petroleum and hydroelectric development further north (Fig. 1). Consequently, my measures of human activity covary strongly with the natural environmental gradient in Canada (Table 5). From 35% to 68% of the variation in road density and from 79% to 87% of the variation in natural cover is explained by precipitation, temperature, and vegetation type (ANCOVA, $p<10^{-5}$), depending on the scale (Table 5).

Protected area status (i.e., park area) covaries less strongly (9% to 36%) with the environmental gradient than do measures of human activity (ANCOVA, $p<10^{-5}$). Park area is weakly collinear with road density (Spearman rank correlation, -0.16 to -0.42, Table 3) and extent of natural cover (Spearman rank correlation, 0.25 to 0.56, Table 3).

Ecosystem Function, Anthropogenic Activity, and Spatial Scale

The purpose of my study was to determine the extent to which indices of ecosystem function are related to measures of human activity and protected area status across spatial scales. I found that, without controlling for climate or vegetation type, from 51% to 57% of the variation in NDVI and from 60% to 67% of the variation in TIR, depending on spatial scale, is potentially related to road density, extent of natural cover, and park area (human only r^2, Table 6).

Controlling for climate and vegetation type masks some, perhaps much, of the effect of human activities because of their collinearity with climate. Nonetheless, when considered together, human activity (road density and natural cover) and protected area status still account for significant amounts of the residual variation in NDVI (14% to 67%) and TIR (10% to 55%) (Table 6). The absolute amount of residual variation in NDVI and TIR that is related to my measures of human activity and to protected area status after controlling for climate and vegetation type is small (1% to 7%) but statistically significant (Table 6).

Overall, a model that includes human activity, protected area status, and natural environmental variables explains nearly all the variation in NDVI (85% to 96%) and TIR (91% to 97%) (natural + human r^2, Table 6). All relationships become stronger as spatial scale increases.

Road density and natural cover explain different proportions of the variation in NDVI and TIR. More of the residual variation in NDVI is explained by road density (6% to 36%) than by extent of natural cover (8% to 33%) (Table 7). By comparison, TIR is more strongly related to natural cover (7% to 30%) than to road density (2% to 27%) (Table 7). Residual variation in TIR is not significantly related to road density at the coarsest spatial scale for one of four replicates (Table 8).

Protected area status explains a significant amount of residual variation in NDVI and TIR even after controlling for both climate and human activities (road density and natural cover). From 3% to 37% of the residual variation in NDVI and from 1% to 19% of the variation in TIR is related to protected area status (park area) (Appendix B). For TIR, park area is non-significant in three of four replicates at the coarsest spatial scale (Appendix B).

Finally, I found that spatial autocorrelation decreases with increasing spatial scale. Spatial autocorrelation in the total model residuals for both NDVI and TIR is high at fine spatial scales ($I = 0.69$) and fluctuates around zero at the coarsest spatial scale. For the smallest quadrat sizes (225 km^2 and 675 km^2), all variables remain significant in the model even when sample size is reduced by 99% ($n=60$, $p<0.001$; $n=20$, $p<0.001$). Moran's I becomes smaller more rapidly at quadrat sizes of 2025 km^2 and 6075 km^2. At this scale, all model variables still remain significant even when sample size is reduced by 90% and 95%, respectively ($n=70$, $p<0.001$; $n=10$, $p<0.05$). At the coarsest spatial scale, Moran's I fluctuates around zero, so spatial autocorrelation was not a concern. The patterns between spatial scales are qualitatively similar. Therefore it is highly unlikely that spatial autocorrelation creates any patterns, given that no spatial autocorrelation exists at the coarsest spatial scale.

Measurement error in NDVI and TIR does not differ markedly among spatial scales. Interannual variation in NDVI is 1.18×10^{-4} to 1.33×10^{-4} (unitless), while interannual variation in TIR is 1646 $(°K)^2$ to 2182 $(°K)^2$. Across spatial scales, interannual variation in NDVI and TIR differs by 20% and 30%, respectively.

Direction of the Relationships

I first examined the variation in NDVI and TIR across the range of human activity and protected area status in southern Canada, before controlling for climate and vegetation type. Across vegetation types in general, NDVI decreases from approximately 0.65 to 0.55 (unitless) and TIR increases from 5700°K to 5900°K across road density values ranging from 0.25 to 0.40 $(km/km^2)^{0.2}$ (Fig. 8). Based on net primary productivity-NDVI relationships in the literature (Goward et al. 1985), a change in NDVI from 0.65 to 0.55 (approximately 1405 g $C/m^2/yr$ to 1196 g $C/m^2/yr$) represents a 15% reduction in net primary productivity across the range of road density values examined. In rangeland/pasture, grassland, and grain/canola, NDVI and TIR show the opposite response to increasing road density: NDVI increases from approximately 0.32 to 0.52 and TIR decreases from 6070°K to 5900°K (Fig. 8). This difference disappears, however, after controlling for climate (Fig. 9).

NDVI and TIR respond similarly to increasing extent of natural cover (i.e., decreasing amount of agricultural land), irrespective of vegetation type. NDVI increases noticeably from approximately 0.44 to 0.58 and TIR decreases rapidly from 6050°K to 5850°K, which corresponds to an increase in natural cover of approximately 5600 km^2, or 30% of the quadrat area at the coarsest spatial scale. Beyond 30% natural coverage, NDVI levels off, while TIR continues to decrease, albeit less rapidly. Over the entire range of protected area status, which varies from 0 to 0.92 $(km^2/km^2)^{0.2}$. NDVI increases continuously and TIR decreases (Fig. 8).

In general, ecosystems with more intense human activity are less productive (lower NDVI) and hotter. After controlling for climate and vegetation type, NDVI and TIR residuals are inversely related to each other in nearly all vegetation types (Pearson correlation, $p<0.05$). At the coarsest spatial scale, NDVI covaries positively with extent of natural cover ($p<10^{-5}$) and amount of park area ($p<10^{-5}$) and negatively with road density ($p<10^{-5}$), after controlling for climate and vegetation type (Fig. 9). Relationships are weak and non-significant at finer spatial scales. Visual inspection of NDVI variation reveals the striking difference between intensive agricultural areas in central and southern Canada (yellow, orange) and northern boreal and mixed forests (green) (Fig. 2).

Similarly, ecosystems with more human activity tend to radiate more heat: TIR is positively related to road density ($p<10^{-4}$) and covaries negatively with natural cover ($p=0.034$) and park area ($p=0.035$) at the coarsest spatial scale (Fig. 9). As with NDVI, areas of intense human impact can be visually detected as hotter (dark red) than more natural areas (light red), even at a coarse resolution. This pattern is visually evident in agricultural areas, such as the Okanagan Valley of British Columbia (1), small patches of agriculture in areas of boreal forest north of Lake Huron (2), and southern Ontario and the Eastern Townships of Québec (3) (Fig. 3). The James Bay-LaGrande hydroelectric project (4) is also hotter than the surrounding land (Fig. 3). These relationships are weak at fine spatial scales (data not shown) and become stronger at broader spatial scales for both NDVI and TIR (Fig. 9).

Vegetation-Specific Relationships

To a degree, both NDVI and TIR show vegetation-specific responses to human activities. In most vegetation types, NDVI is negatively related to road density and positively related to park area and natural cover (Table 9; see Appendix B for representative residual plots of NDVI versus road density, by vegetation type). However, NDVI is positively related to road density in two western agricultural classes (grassland/rangeland and pasture) and negatively related to park area in coniferous forest classes. NDVI is most strongly related to human activity in pasture/forest/cropland, an eastern agricultural class, and mixed/open deciduous forest.

Similarly, TIR is nearly always positively related to road density and negatively related to park area and natural cover (Table 9; see Appendix B for representative residual plots of TIR versus road density, by vegetation type). The exceptions to this general trend occur in grassland/rangeland and pasture. Interestingly, within all forest classes and the eastern agricultural class, pasture/forest/cropland, the relationships between TIR and park area and natural cover are mostly weak and equivocal in that the slopes can be either positive or negative within individual classes.

Discussion

Ecologists have expressed concern about the possibility of collapse of ecosystem function due to continuing exploitation of species and habitats. Clearly this can happen at fine spatial scales: pavement has neglible productivity. However, I am unaware of any study that has examined ecosystem function at landscape to regional scales along a continuous gradient of human activity. I evaluated whether two remotely sensed indices of ecosystem function, primary productivity (NDVI) and evapotranspiration (TIR), are statistically related to measures of anthropogenic activity. Clearly, these are not the only relevant aspects of ecosystem function; rather, they are two important aspects that can be monitored at the scales of interest.

I found that much of the variation in my indices of ecosystem function is related to road density, natural cover, and protected area status, even after controlling for climate and vegetation type. This demonstrates that, across a wide variety of vegetation types and ecological conditions, ranging from 100% natural cover to nearly 100% urbanized, patterns of ecosystem function are statistically related to levels of anthropogenic activity. Across vegetation types, reduced natural cover is associated with ecosystems that are less productive and, to a lesser extent, re-radiate more heat (i.e., evaporate less water). This is consistent with findings from whole-watershed studies in the Hubbard Brook Experimental Forest (Bormann and Likens 1996) and comparisons of NDVI and per cent vegetation cover (Purevdorj et al. 1998; Kant and Badarinth 2000; Roy 1997).

Ecosystem function-human activity relationships are most apparent at coarser spatial scales. At local spatial scales, differences in microclimate, soil type, etc., increase the variability in NDVI and TIR (Dash et al. 2002; Waring and Running 1998), but these effects presumably average out when ecosystem function is integrated over broader geographic areas. Hence a greater proportion of the variation in NDVI and TIR can be related to human activity at coarser spatial scales. TIR is less strongly related to measures of human activity than NDVI, possibly because TIR is more variable locally than regionally (Luvall and Holbo 1991).

I found no obvious threshold in the response of NDVI or TIR to increasing intensity of human activity. According to Ehrlich and Ehrlich's (1981) rivet hypothesis, there exists a threshold of biodiversity below which ecosystems lose the self-organisation that enables them to provide ecological services. Areas of greatest human impact are inferred to undergo the most severe rates of biodiversity loss (Czech et al. 2000), but I did not detect any sudden decrease in either of my measures of ecosystem function as inferred from the rivet hypothesis. Clearly, dramatic changes in ecosystems can occur at finer spatial scales, or even at broad scales in response to specific perturbations such as contamination with highly toxic industrial pollutants (e.g., areas downwind of the Sudbury nickel smelters, or downstream of humans and industry in Lake Erie; Freedman 1995). I did not examine the ecological effects in urban areas because they were masked out from the study region, although densely populated urban areas are a clear example of severely disturbed ecosystems. At broad spatial scales, ecosystem function declines gradually, rather than abruptly, along a gradient of human activity.

The changes in ecosystem function associated with urbanization and agriculture are substantial. The magnitude of difference between NDVI and TIR in areas of least human activity versus areas of greatest activity is approximately 0.05 units in seasonally-averaged NDVI and 20°K in seasonally-integrated TIR, after controlling for climate and vegetation type (Fig. 9). In many cases, this is comparable to the among-vegetation type differences in mean NDVI and TIR (Table 1). According to an empirically defined relationship between NDVI and net primary productivity in the literature (Goward et al. 1985), this is equivalent to a 15% reduction in net primary productivity across all vegetation types.

A map of observed ecosystem function (as measured by NDVI) minus the expected value (estimated from climate and vegetation type) shows areas where function is unexpectedly high or low (Fig. 10). I do not have direct evidence about the causes of these deviations. However, nearly all negative deviations appear to be associated with recognized human perturbations: e.g., logging (northern Vancouver Island and parts of northern British Columbia), hydroelectric development (northern Québec and Labrador), industrial pollution (Sudbury Ontario, Asbestos Québec, and Sydney/Glace Bay Nova Scotia), and intensive agriculture (southern Ontario). Low spots are also seen through the Bow River Valley in Banff National Park, Alberta, where human development is considered a major ecological threat (Parks Canada Agency 2000), and immediately west of the mountain parks. NDVI also deviates from expected in New Brunswick and Nova Scotia, which may be related to spruce budworm infestation and/or logging (D. Currie, personal observation.).

Different ecosystem types generally respond in a similar way (i.e., reduced productivity and evapotranspiration) to increasing road density and decreasing natural cover, after controlling for climate. Within agricultural types, increasing amount of treed land (i.e., from grain/canola to woodland-cropland) is associated with greater productivity and evapotranspiration (Table 9). Overall, forests are more productive than agricultural land as measured by seasonally-averaged NDVI (Table 1). Because forests and agricultural crops have very dissimilar surface properties and therefore different energy budgets, this leads to dramatically different rates of evapotranspiration (Quattrochi and Luvall 1999). Due to the obvious differences that exist between species in terms of the amount of evapotranspiration per unit of photosynthetic output, water use per unit of biomass is not constant across species. For example, agricultural ecosystems dominated by corn (which uses the C_4 photosynthetic pathway and therefore transpires less water per unit of biomass, Raven et al. 1986) are vastly different from most ecosystems found in Canada, which consist of C_3 plants and therefore have tend to have higher rates of evapotranspiration per unit of biomass. Striking differences in the ratio of evapotranspiration to productivity also exist between coniferous and deciduous forests, as well as primary versus secondary growth forests (Raven et al. 1986). These vegetation-specific responses, however, must be conservatively interpreted. Although I used the best coarse-resolution land cover data available, these data are most appropriate for analysis over a broad spatial extent. I make no inference regarding local or sub-pixel level analysis due to the heterogeneous composition of both pixels and quadrats (Cihlar et al. unpublished).

Interestingly, greater protected area status is associated with higher productivity and, to a lesser extent, with higher evapotranspiration. This could reflect a beneficial effect of protected status on ecosystem function. Alternatively, it is possible that parks were established in areas with relatively high NDVI and low TIR. However, the latter seems unlikely. Historically, park creation was driven by recreational interest rather than being guided by ecological principles. For example, Banff National Park began as a resort for the wealthy after railway workers discovered hot springs in 1883 (Searle 2000). Parks tended to be established in scenic spots (what have been called "rock and ice parks") rather than in particularly productive areas, which are prized for agriculture. At the minimum, my results are consistent with the hypothesis that protected area status may help to maintain higher levels of primary productivity and evapotranspiration.

I assumed that, across Canada, road density is a good indicator of the spatial variability of human activities in general. To test this assumption, I compared my measure of road density with Sanderson et al.'s (2002) "human footprint" by extracting data with each sampling grid as before. Sanderson et al. included multiple aspects of human activity in their human footprint, such as population density, land transformation, accessibility (rivers, railways, roads), and electrical power infrastructure, but their human footprint is essentially a linear disturbance metric. I found that road density is strongly correlated with the human footprint in Canada (Pearson correlation, $r = 0.72$ to $r = 0.92$, depending on spatial scale). The correlation between roads and human footprint is not surprising: roads show a high degree of association with population growth, agricultural intensification, electrical power infrastructure, and increased species endangerment (Schindler 1990; Czech et al. 2000; McKinney 2002).

It is not likely that my estimates of human impact are lower than they might otherwise be as a consequence of low human population density in Canada compared to other parts of North America. The human footprint values in major urban centres in Canada and the U.S. are comparable (Sanderson et al. 2002). Thus, the range of human influence in Canada is not smaller than in the U.S. and it is unlikely that a larger effect of human activity would be detected in the U.S.

Not surprisingly, I found that NDVI and TIR are strongly related to climate, which is consistent with empirical studies of NDVI and climatic gradients at continental and global scales (Goward et al. 1985; Ichii et al. 2002). While climate generally yields the greatest influence on spatial patterns of NDVI and TIR, it may become secondary in its importance in areas of intense human activity. For example, Paruelo et al. (2001) performed a multi-year analysis of seasonally integrated NDVI in the short-grass steppe of eastern Colorado, a study area with a smooth climatic gradient and homogeneous potential vegetation. Land use, indicative of the intensity of human activity, was more important in explaining regional differences in NDVI dynamics than climatic factors in this single habitat type.

Separating the large natural variability of ecosystems from that associated with human activity is difficult, parituclarly in Canadian data because of the high collinearity between climate and human activity. Consequently, a large proportion of the variability in NDVI (and TIR) can be attributed to either natural *or* human factors (Fig. 11). The only way to eliminate this problem would be to select a study area where human activity was distributed independently of climate. The consequences of multicollinearity are that regression coefficients may have unexpected signs or a large change in partial regression coefficients can occur with the addition or removal of a variable from the model (Zar 1999). Occasionally, individual terms do become non-significant at the coarsest spatial scale due to the high collinearity between climate and road density. When tested individually in general linear models, human activity variables and protected area status are nearly always statistically significant (Table 7).

My study did not address structural properties of ecosystems, although these may be more sensitive to human-induced changes than ecosystem functions (Schindler 1990; Asner et al. 1998). First-order ecosystem processes, such as photosynthesis, transpiration, and decomposition, are often relatively insensitive to forest species composition (Waring and

Running 1998). Therefore rates of ecosystem productivity and water cycling may remain relatively undisturbed in spite of changes to composition.

Spatial autocorrelation in model residuals is unlikely to have significantly affected hypothesis testing in this study. At the finest spatial scale, Moran's I was non-negligible. However, the data could be reduced to 1% of the total sample size without affecting the significance of my results. At coarser spatial scales, spatial autocorrelation gradually diminished and disappeared at the largest quadrat size. Measurement error in NDVI and TIR was relatively stable across spatial scales and likely does not influence the interpretation of my results.

Conclusion

My empirical modelling approach examined ecological changes at scales significantly larger than is possible using traditional field data (on which most of my existing knowledge is based), yet closer to the scale of major human impacts. I found that much of the residual variation in NDVI and TIR is related to measures of human impact, even after controlling for climate. While ecosystem function changes substantially across the range of human activity, I found no evidence of a threshold effect in the response of ecosystem functions. Regions where observed NDVI deviates greatly from expected values—particularly in areas associated with logging, industrial pollution, and hydroelectric development—can be detected visually. Across different vegetation types, primary productivity and evapotranspiration increase as road density decreases and natural cover increases. In addition, protected areas may, at the minimum, help to maintain ecosystem function, particularly primary productivity. These relationships are strongest at coarse spatial scales and are generally consistent within different vegetation types. Road density appears to be a good indicator of the overall intensity of human activities in Canada. The magnitude of these effects along the entire gradient of human activity is substantial.

Literature Cited

Asner, G. P., Braswell, B. H., Schimel, D. S., and C. A. Wessman. 1998. Ecological research needs from multiangle remote sensing data. Remote Sensing of Environment 63:155-165.

Balmford, A., Bruner, A., Cooper, P., Costanza, R., Farber, S., Green, R. E., Jenkins, M., Jefferiss, P., Jessamy, V., Madden, J., Munro, K., Myers, N., Naeem, S., Paavola, J., Rayment, M., Rosendo, S., Roughgarden, J., Trumper, K., and R. K. Turner. 2002. Economic Reasons for Conserving Wild Nature. Science 297: 950-953.

Bertollo, P. 1998. Assessing ecosystem health in governed landscapes: A framework for development core indicators. Ecosystem Health 4(1): 33-51.

Bormann, F. H. and G. E. Likens. 1994. Pattern and process in a forest ecosystem. Springer-Verlag, New York.

Box, E. O., Holben, B. N., and V. Kalb. 1989. Accuracy of the AVHRR Vegetation Index as a predictor of biomass, primary productivity and net CO_2 flux. Vegetatio 80: 71-89.

Budykov, M. I. 1974. Climate and life. Academic Press, Inc., London.

Cihlar, J., Beaubien, J., and R. Latifovic. 2002. Land cover of Canada 1998. Special Publication, NBIOME Project. Produced by the Canada Centre for Remote Sensing and the Canadian Forest Service, Natural Resources Canada. Available from the Canada Centre for Remote Sensing, Ottawa, Ontario.

Cihlar, J. Latifovic, R., Beaubien, J., Guindon, B., and M. Palmer. In press. TM-based accuracy assessment of a land cover product for Canada derived from SPOT VEGETATION data. Canadian Journal of Remote Sensing.

Cihlar J., Chen, J. M., Li, Z. , Latifovic, R., Fedosejevs, G., Adair, M., Park, W. M., Fraser R., Trishchenko, A., Guindon, B., Stanley, D., and D. Morse. 2002. GeoComp-n, an advanced system for the processing of coarse and medium resolution satellite data. Part 2: biophysical products for northern ecosystems. Canadian Journal of Remote Sensing 28(1): 21-44.

Cihlar, J., St.-Laurent, L., and J. A. Dyer. 1991. Relation between the normalized difference vegetation index and ecological variables. Remote Sensing of Environment 35: 279-298.

Costanza, R. and M. Mageau. 1999. What is a healthy ecosystem? Aquatic Ecology 33(1): 105-115.

Czajkowski, K. P., Mulhern, T., Goward, S. N., Cihlar, J., Dubayah, R. O., and S. D. Prince. 1997. Biospheric environmental monitoring at BOREAS with AVHRR observations. Journal of Geophysical Research 102(D24): 29,651-29662.

Czech, B., Krausman, P. R., and P. K. Devers. 2000. Economic associations among causes of species endangerment in the United States. Bioscience 50(7): 593-601.

Daily, G. C. 1997. Nature's services: societal dependence on natural ecosystems. Island Press: Washington, D. C.

Dash, P., Göttsche, F.-M., Olsesen, F.-S. and H. Fischer. 2002. Land surface temperature and emissivity estimation from passive sensor data: theory and practice—current trends. International Journal of Remote Sensing 23(13): 2563-2594.

DMTI Spatial. Canmap Streetfiles 5.1. [computer file]. Markham, Ontario: DMTI Spatial, 2001.

Ehrlich, P. R. and A. H. Ehrlich. 1981. Extinction: the causes and consequences of the disappearance of species. Random House, New York.

Forman, R. T. T. 2000. Estimate of the area affected ecologically by the road system in the united states. Conservation Biology 14(1): 31-35.

Freedman, B. 1995. Environmental Ecology, Second Edition. Academic Press, New York.

Fung, T. and W. Siu. 2000. Environmental quality and its changes, an analysis using NDVI. International Journal of Remote Sensing 21(5): 1011-1024.

Gibson, C. C., Ostrom, E., and T. K. Ahn. 2000. The concept of scale and the human dimensions of global change: a survey. Ecological Economics 32: 217-239.

Goldstein, P. Z. 1999. Functional ecosystems and biodiversity buzzwords. Conservation Biology 13(2): 247-255.

Goward, S. N., Tucker, C. J., and Dye, D. G. 1985. North American vegetation patterns observed with the NOAA-7 advanced very high resolution radiometer. Vegetatio 64:3-14.

Huston, M. A. 1997. Hidden treatments in ecological experiments: re-evaluating the ecosystem function of biodiversity. Oecologia 110: 449-460.

Ichii, K., Kawabata, A., and Y. Yamaguchi. 2002. Global correlation analysis for NDVI and climatic variables and NDVI trends: 1982-1990. International Journal of Remote Sensing 23(18): 3873-3878.

Kant, Y and K. V. S. Badarinth. 2000. Studies on land surface temperature over heterogeneous areas using AVHRR data. International Journal of Remote Sensing 21(8): 1749-1756.

Kay, J., Allen, T., Fraser, R., Luvall, J., and R. Ulanowicz. 2002. Can we use energy based indicators to characterize and measure the status of ecosystems, human, disturbed and natural? Proceedings of the international workshop: Advances in Energy Studies: exploring supplies, constraints and strategies, Porto Venere, Italy, 23-27 May, 2000 pp. 121-133.

Kerr, J. T. and J. Cihlar. 2003. Land use and cover with intensity of agriculture for Canada from satellite and census data. Global Ecology and Biogeography 12(2): 161-172.

Kok, K. and A. Veldekamp. 2001. Evaluating impact of spatial scales on land use pattern analysis in Central America. Agriculture, Ecosystems and Environment 85: 205-221.

Krausmann, F. 2001. Land use and industrial modernization: an empirical analysis of human influence on the functioning of ecosystems in Austria 1830-1995. Land Use Policy 18: 17-26.

Kremen, C., Williams, N. M. and R. W. Thorp. 2002. Crop pollination from native bees at risk from agricultural intensification. Proceedings of the National Academy of Sciences 99(26): 16812-16816.

Latifovic, R. 2002. Special Publication, NBIOME Project. Natural Resources Canada, Canada Centre for Remote Sensing. Ottawa, ON.

Lawton, J. H. and V. K. Brown. 1993. Redundancy in ecosystems. In E.-D. Schulze and H. A. Mooney (eds.). *Biodiversity and ecosystem function*. Springer-Verlag, New York.

Lieth H. (1975) Modeling the primary production of the world. In H Leith and R. H. Whittaker (eds.). *Primary Production of the Biosphere*. Springer-Verlag, New York.

Levin, S. A. 1992. The problem of pattern and scale in ecology. Ecology 73(6): 1943-1967.

Loreau, M. Naeem, S., Inchausti, P., Bengtsson, J., Grime, J. P., Hector, A., Hooper, D. U., Huston, M. A., Raffaelli, D., Schmid, B., Tilman., D., and D. Wardle. 2001. Biodiversity and ecosystem functioning: current knowledge and future challenges. Science 294: 804-808.

Luvall, J. C. and H. R. Holbo. 1991. Thermal remote sensing methods in landscape ecology. In M. G. Turner and R. H. Gardner (eds.). *Quantitative methods in landscape ecology*. Springer-Verlag, New York.

McKenney, D. W., Hutchison, M. F., Kesteven, J. L., and L. A. Venier. 2001. Canada's plant hardiness zones revisited using modern climate interpolation techniques. Canadian Journal of Plant Science 81:129-143.

McKinney, M. L. 2002. Urbanization, biodiversity and conservation. Bioscience 52(10): 883-889.

McNaughton, S. J., Oesterheld, M., Frank, D. A., and K. J. Williams. 1989. Ecosystem-level patterns of primary productivity and herbivory in terrestrial habitats. Nature 341: 142-144.

Naeem, S. 2002. Ecosystem consequences of biodiversity loss: the evolution of a paradigm. Ecology 83(6): 1537-1552.

Perakis, S. S. and L. O. Hedin. 2002. Nitrogen loss form unpolluted South American forests mainly via dissolved organic compounds. Nature 415: 416-419.

Parks Canada Agency. 2000. "Unimpaired for future generations"? Protecting ecological integrity with Canada's national parks. Vol. I "A call to action." Vol. II "Setting a new direction for Canada's national parks." Report of the Panel on the Ecological Integrity of Canada's National Parks. Ottawa, ON.

Paruelo, J. M., Burke, I. C., and W. K. Lauenroth. 2001. Land-use impact on ecosystem functioning in eastern Colorado, USA. Global Change Biology 7: 631-639.

Purevdorj, Ts., Tateishi, R., Ishiyama, T., and Y. Honda. 1998. Relationships between percent vegetation cover and vegetation indices. International Journal of Remote Sensing 19(18): 3519-3535.

Quattrochi, D. A. and J. C. Luvall. 1999. Thermal infrared remote sensing for analysis of landscape ecological processes: methods and applications. Landscape Ecology 14: 577-598.

Rapport, D. J., Whitford, W. G., and M. Hilden. 1998. Common patterns of ecosystem breakdown under stress. Environmental Monitoring & Assessment 51(1): 171-178.

Raven, P. H., Evert, R. F., and S. E. Eichhorn. 1986. Biology of plants, fourth edition. Worth Publishers, Inc., New York.

Roy, D. P. 1997. Investigation of the maximum Normalized Difference Vegetation Index (NDVI) and the maximum surface temperature (Ts) AVHRR compositing procedures for the extraction of NDVI and Ts over forest. International Journal of Remote Sensing 18(11): 2383-2401.

Rosenzweig, M.L. 1968. Net primary productivity of terrestrial communities: prediction from climatological data. American Naturalist 102: 67-74.

Running, S. W. and R. R. Nemani. 1988. Relating seasonal patterns of the AVHRR vegetation index to simulated photosynthesis and transpiration of forests in different climates. Remote Sensing of Environment 24: 347-367.

Sanderson, E. W., Jaiteh, M., Levy, M. A., Redford, K. H., Wannebo, A. V., and G. Woolmer. 2002. The human footprint and the last of the wild. Bioscience 52(10): 891-904.

Schindler, D. W. 1990. Experimental perturbations of whole lakes as tests of hypotheses concerning ecosystem structure and function. Oikos 57:25-41.

Schläpfer, F., B. Schmid, and I. Seidl. 1999. Expert estimates about effects of biodiversity on ecosystem processes and services. Oikos 84(2): 346-352.

Schneider, E. D. and J. J. Kay. 1994. Complexity and thermodynamics: towards a new ecology. Futures 26(6): 626-647.

Seabloom, E. W., Dobson, A. P., and D. M. Stoms. 2002. Extinction rates under nonrandom patterns of habitat loss. Proceedings of the National Academy of Science USA 99(17): 11229-11234.

Searle, Rick. 2000. Phantom parks: the struggle to save Canada's national parks. Key Porter Books, Toronto.

Sellers, P. J., Berry, J. A., Collatz, G. J., Field, C. B., Hall, F. G. 1992. Canopy reflectance, photosynthesis and transpiration. III. A reanalysis using improved leaf models and a new canopy integration scheme. Remote Sensing of Environment 42(3): 187-216.

Sellers, P.J. 1985. Canopy reflectance, photosynthesis and transpiration. International Journal of Remote Sensing 6:1335-1372.

Smith, F. D. M., Daily, G. C., and P. R. Ehrlich. 1995. Human population dynamics and biodiversity loss. In T. M. Swanson (ed.) *The economics and ecology of biodiversity decline*. Cambridge University Press, Cambridge, UK. Pp. 125-141.

Statistics Canada. 2002. 2001 Census dictionary. Statistics Canada, Census Operations. Ottawa, ON.

Stoms, D. M. and W. W. Hargrove. 2000. Potential NDVI as a baseline for monitoring ecosystem functioning. International Journal of Remote Sensing 21(2): 401-407.

Trombulak, S. C. and C. A. Frissell. 2000. Review of ecological effects of roads on terrestrial and aquatic communities. Conservation Biology 14(1): 18-30.

Vitousek, P., Ehrlich, P. R., Erhlich, A. H., and P. Matson. 1986. Human appropriation of the products of photosynthesis. Bioscience 36: 368-373.

Wackernagel, M., Schulz, N. B., Deumling, D., Linares, A. C., Jenkins, M., Kapos, V., Monfreda, C., Loh, J., Myers, N., Norgaard, R., and J. Randers. 2002. Tracking the ecological overshoot of the human economy. Proceedings of the National Academy of Sciences USA 99(14): 9266-9271.

Waring, R. H. and S. W. Running. 1998. Forest ecosystems: analysis at multiple scales. Academic Press, New York.

Wright, D. H. 1990. Human impacts on energy flow through natural ecosystems, and implications for species endangerment. Ambio 19(4): 189-194.

Zar, J. H. 1999. Biostatistical analysis, 4th Edition. Prentice Hall, New Jersey.

Table 1. Summary of mean NDVI (normalized difference vegetation index) and TIR (thermal infrared radiation) within each vegetation type, as well as the range of climate variables. Mean Pearson correlation coefficients for ecosystem function—NDVI and TIR—and $(\text{precipitation})^{0.2}$ and temperature relationships are also presented. NDVI and TIR show statistically indistinguishable relationships with climate within vegetation types. All correlations are statistically significant ($p<0.001$) and are based on 225 km^2 quadrats.

i. ecosystem function: NDVI

vegetation type	mean NDVI	precipitation range	temperature range	precipitation r	temperature r
grassland/rangeland (W)*	0.32	2.9 – 3.1	10.9 – 13.4	-0.32	0.53
grain/canola (W)[a]	0.44	2.9 – 3.7	9.0 – 13.7	-0.56	0.79
pasture (W)	0.44	2.9 – 3.5	8.6 – 13.4	-0.61	0.83
low density pasture (W)	0.51	3.0 – 3.4	8.9 – 12.8	-0.60	0.46
woodland-agriculture (W)	0.53	3.1 - 3.8	8.1 - 13.9	-0.23	0.54
corn/soybean[b]	0.54	3.3 – 3.8	9.3 – 16.5	-0.65	0.32
pasture/forest/cropland (E)[c]	0.58	3.4 – 3.8	9.6 – 16.7	-0.31	0.28
low density conifer. forest[d]	0.52	2.9 – 3.8	3.3 – 14.5	0.39	-0.075
conifer. forest w/ broadleaf[e]	0.58	2.9 – 4.3	3.6 – 13.7	0.64	0.25
mixed/open decid. forest	0.62	3.0 – 4.2	5.2 – 16.1	0.69	0.39

ii. ecosystem function: TIR

vegetation type	mean TIR	precipitation range	temperature range	precipitation r	temperature r
grassland/rangeland (W)	6064.	2.9 – 3.1	10.9 – 13.4	0.62	-0.55
grain/canola (W)	5960.	2.9 – 3.7	9.0 – 13.7	0.73	-0.68
pasture (W)	5981.	2.9 – 3.5	8.6 – 13.4	0.76	-0.80
low density pasture (W)	5920.	3.0 – 3.4	8.9 – 12.8	0.68	-0.44
corn/soybean	5913.	3.3 – 3.8	9.3 – 16.5	0.81	-0.35
woodland-agriculture (W)	5889.	3.1 - 3.8	8.1 - 13.9	0.62	-0.13
pasture/forest/cropland (E)	5876.	3.4 – 3.8	9.6 – 16.7	0.86	-0.57
low density conifer. forest	5835.	2.9 – 3.8	3.3 – 14.5	0.75	-0.53
conifer. forest w/ broadleaf	5807.	2.9 – 4.3	3.6 – 13.7	0.63	-0.26
mixed/open decid. forest	5825.	3.0 – 4.2	5.2 – 16.1	0.52	-0.32

*(W) and (E) indicate that a vegetation type includes only quadrats west or east of 90°W, i.e., western versus eastern agriculture

Vegetation types consist of the following land use classes: [a]Low moisture grain, grain/canola, and canola, [b]corn soybean mix with pasture and corn/soybean; [c]pasture, grain/canola, and woodland-agriculture; [d]northern conifers and very low density conifers with various understory or barren; and [e]conifers/low density conifers and northern conifers

Table 2. The mean, range, and standard deviation (s.d.) among quadrats of the ecosystem function, climate, and human activity variables used in this study.

variable	quadrat size (km^2)*	mean	minimum	maximum	s.d.
NDVI (seasonally-averaged normalized difference vegetation index) (unitless)	225[a]	0.53	0.27	0.70	0.09
	675[b]	0.53	0.28	0.68	0.09
	2025[c]	0.53	0.28	0.67	0.09
	6075[d]	0.53	0.28	0.68	0.09
	18225[e]	0.53	0.32	0.66	0.08
TIR (seasonally-integrated thermal infrared radiation) (°K)	225	5882.	5578.	6103.	78.
	675	5883.	5614.	6097.	77.
	2025	5882.	5628.	6090.	77.
	6075	5884.	5674.	6080.	77.
	18225	5880.	6073.	6063.	76.
$(\text{precipitation})^{0.2}$ (mm)	225	3.38	2.87	4.28	0.24
	675	3.38	2.90	4.27	0.24
	2025	3.39	2.95	4.23	0.24
	6075	3.39	2.97	3.99	0.24
	18225	3.40	2.99	3.85	0.24
temperature (°C)	225	11.1	3.3	16.7	1.7
	675	11.1	3.6	16.5	1.6
	2025	11.2	4.0	16.3	1.6
	6075	11.2	4.8	16.0	1.6
	18225	11.1	5.4	14.8	1.6
$(\text{road density})^{0.2}$ (km/km^2)	225	0.303	0.251	0.523	0.035
	675	0.302	0.251	0.505	0.033
	2025	0.301	0.251	0.462	0.032
	6075	0.300	0.251	0.423	0.030
	18225	0.299	0.252	0.390	0.030
natural cover† (km^2)	225	102.	0.	238.	94.
	675	297.	0.	723.	274.
	2025	862.	0.	2099.	776.
	6075	2449.	3.	6203.	2192.
	18225	7307.	52.	17750.	6153.
$(\text{park area})^{0.2}$ (km^2/km^2)	225	0.16	0.00	1.00	0.28
	675	0.24	0.00	1.00	0.30
	2025	0.35	0.00	1.00	0.28
	6075	0.44	0.00	0.95	0.23
	18225	0.51	0.00	0.96	0.24

*Each quadrat set has the following sample size (averaged over four replicates): a=6449; b=2225; c=762; d=274; e=96.

†Map projection caused occasional distortion, resulting in quadrats slightly but insignificantly larger than stated size.

Table 3. Mean Spearman rank correlation coefficients (pooled over replicates) among independent variables used in this study. Variables were transformed to yield approximately symmetrical distributions using the following transformations: $(\text{precipitation})^{0.2}$, temperature (untransformed), $(\text{road density})^{0.2}$, natural cover (untransformed), and $(\text{park area})^{0.2}$.

quadrat size (km^2)		variables: precipitation	temperature	road density	natural cover	park area
225	precipitation	1.00				
	temperature	-0.038	1.00			
	road	0.064	0.48	1.00		
	natural cover	0.55	-0.48	-0.37	1.00	
	park area	0.14	-0.11	-0.16	0.25	1.00
675	precipitation	1.00				
	temperature	-0.044	1.00			
	road density	0.071	0.54	1.00		
	natural cover	0.55	-0.50	-0.42	1.00	
	park area	0.16	-0.16	-0.26	0.31	1.00
2025	precipitation	1.00				
	temperature	-0.033	1.00			
	road density	0.10	0.56	1.00		
	natural cover	0.55	-0.51	-0.45	1.00	
	park area	0.20	-0.23	-0.36	0.41	1.00
6075	precipitation	1.00				
	temperature	-0.047	1.00			
	road density	0.11	0.57	1.00		
	natural cover	0.56	-0.53	-0.47	1.00	
	park area	0.28	-0.28	-0.43	0.52	1.00
18225	precipitation	1.00				
	temperature	-0.027	1.00			
	road density	0.17	0.61	1.00		
	natural cover	0.52	-0.57	-0.51	1.00	
	park area	0.37	-0.28	-0.42	0.56	1.00

Table 4. Summary of general linear model results ($r^2 \pm 95\%$ C. I.) showing the dependence of NDVI (normalized difference vegetation index) and of TIR (thermal infrared radiation) on climate ($precipitation^{0.2}$ + temperature + $precipitation^{0.2}$*temperature), vegetation type (10-class categorical variable), or both, where *n* represents the average number of quadrats at each spatial scale. All models and model terms are statistically significant ($p<0.05$).

i. dependent variable: NDVI

quadrat size (km^2)	n	climate r^2	vegetation r^2	climate + vegetation r^2
225	6451	0.69 ± 0.01	0.76 ± 0.02	0.83 ± 0.01
675	2225	0.73 ± 0.02	0.75 ± 0.02	0.84 ± 0.02
2025	762	0.74 ± 0.01	0.77 ± 0.04	0.85 ± 0.01
6075	274	0.77 ± 0.01	0.77 ± 0.04	0.88 ± 0.01
18225	96	0.78 ± 0.01	0.78 ± 0.04	0.89 ± 0.01

ii. dependent variable: TIR

quadrat size (km^2)	n	climate r^2	vegetation r^2	climate + vegetation r^2
225	6451	0.84 ± 0.00	0.76 ± 0.02	0.90 ± 0.01
675	2225	0.87 ± 0.00	0.79 ± 0.04	0.92 ± 0.02
2025	762	0.88 ± 0.00	0.77 ± 0.02	0.92 ± 0.01
6075	274	0.90 ± 0.01	0.79 ± 0.05	0.94 ± 0.01
18225	96	0.91 ± 0.02	0.76 ± 0.02	0.94 ± 0.00

Table 5. Summary of multiple linear regression results ($r^2 \pm 95\%$ C. I.) showing the collinearities between anthropogenic variables (road density, natural cover, and protected area status) and climate and vegetation type. All models are of the following form: anthropogenic variable = $(\text{precipitation})^{0.2}$ + temperature + $(\text{precipitation})^{0.2}$*temperature + vegetation + constant, where *vegetation* represents a categorical variable consisting of 10 land use classes.

quadrat size (km^2)	$(\text{road density})^{0.2}$ r^2	natural cover r^2	$(\text{park area})^{0.2}$ r^2
225	0.35 ± 0.01	0.87 ± 0.00	0.091 ± 0.01
675	0.45 ± 0.01	0.84 ± 0.01	0.14 ± 0.01
2025	0.52 ± 0.02	0.81 ± 0.01	0.18 ± 0.02
6075	0.58 ± 0.01	0.77 ± 0.03	0.25 ± 0.04
18225	0.68 ± 0.04	0.79 ± 0.05	0.36 ± 0.03

Table 6. Summary of general linear model results ($r^2 \pm 95\%$ C. I.) examining the dependence of NDVI (normalized difference vegetation index) and of TIR (thermal infrared radiation) on natural environmental factors (temperature, precipitation, vegetation type) versus anthropogenic variables (road density, extent of natural cover, and park area) across spatial scales, where n represents sample size averaged over four replicates and p represents the significance of the aggregate variation explained by human activity (road density, natural cover) and park area in the total model (natural + human). *Human only* r^2 indicates the variation in NDVI and TIR related to road density, extent of natural cover, and park area *before* controlling for climate and vegetation type. Park area, which is added last in the models, remains statistically significant at all spatial scales ($p<0.05$).

i. dependent variable: NDVI

quadrat size (km^2)	natural r^2	natural+human r^2	human only r^2	human partial r^2	n	p
225	0.83 ± 0.00	0.85 ± 0.00	0.51 ± 0.01	0.14 ± 0.00	6449	$<10^{-5}$
675	0.84 ± 0.01	0.88 ± 0.01	0.53 ± 0.01	0.21 ± 0.01	2225	$<10^{-5}$
2025	0.85 ± 0.01	0.90 ± 0.00	0.53 ± 0.03	0.33 ± 0.05	762	$<10^{-5}$
6075	0.88 ± 0.02	0.94 ± 0.00	0.55 ± 0.03	0.49 ± 0.07	274	$<10^{-5}$
18225	0.89 ± 0.01	0.96 ± 0.00	0.57 ± 0.02	0.67 ± 0.04	96	$<10^{-5}$

ii. dependent variable: TIR

quadrat size (km^2)	natural r^2	natural+human r^2	human only r^2	human partial r^2	n	p
225	0.90 ± 0.00	0.91 ± 0.00	0.60 ± 0.01	0.10 ± 0.01	6449	$<10^{-5}$
675	0.92 ± 0.00	0.93 ± 0.00	0.61 ± 0.01	0.13 ± 0.01	2225	$<10^{-5}$
2025	0.92 ± 0.00	0.94 ± 0.00	0.63 ± 0.02	0.21 ± 0.01	762	$<10^{-5}$
6075	0.94 ± 0.01	0.96 ± 0.01	0.66 ± 0.07	0.34 ± 0.05	274	$<10^{-5}$
18225	0.94 ± 0.01	0.97 ± 0.01	0.67 ± 0.06	0.55 ± 0.12	96	<0.02

Table 7. Summary of general linear model results ($r^2 \pm$ 95% C. I.) examining the dependence of NDVI (normalized difference vegetation index) and of TIR (thermal infrared radiation) on (road density)$^{0.2}$, natural cover, and (park area)$^{0.2}$ across spatial scales, where *vegetation* is a 10-class categorical variable and *p* represents the significance of the variation explained by each of the anthropogenic variables in the following model: (precipitation)$^{0.2}$ + temperature + (precipitation)$^{0.2}$*temperature + vegetation + (road density *or* natural cover *or* park area)*vegetation.

i. dependent variable: NDVI

quadrat size (km^2)	road density partial r^2	p	natural cover partial r^2	p	park area partial r^2	p
225	0.06 ± 0.00	$<10^{-5}$	0.08 ± 0.00	$<10^{-5}$	0.03 ± 0.01	$<10^{-5}$
675	0.10 ± 0.01	$<10^{-5}$	0.12 ± 0.01	$<10^{-5}$	0.05 ± 0.02	$<10^{-5}$
2025	0.14 ± 0.07	$<10^{-5}$	0.17 ± 0.01	$<10^{-5}$	0.11 ± 0.03	$<10^{-5}$
6075	0.20 ± 0.03	$<10^{-5}$	0.24 ± 0.04	$<10^{-5}$	0.20 ± 0.08	$<10^{-5}$
18225	0.36 ± 0.04	$<10^{-3}$	0.33 ± 0.12	$<10^{-2}$	0.37 ± 0.09	$<10^{-3}$

ii. dependent variable: TIR

quadrat size (km^2)	road density partial r^2	p	natural cover partial r^2	p	park area partial r^2	p
225	0.02 ± 0.00	$<10^{-5}$	0.07 ± 0.01	$<10^{-5}$	0.01 ± 0.00	$<10^{-5}$
675	0.04 ± 0.01	$<10^{-5}$	0.07 ± 0.01	$<10^{-5}$	0.02 ± 0.01	$<10^{-5}$
2025	0.06 ± 0.01	$<10^{-5}$	0.10 ± 0.01	$<10^{-5}$	0.05 ± 0.01	$<10^{-3}$
6075	0.12 ± 0.05	<0.007	0.16 ± 0.02	$<10^{-5}$	0.08 ± 0.02	<0.035
18225	0.22 ± 0.13	<0.001, ns	0.25 ± 0.11	<0.013	0.18 ± 0.06	<0.01, ns*

*Individual replicates at the coarsest spatial scale of 18225 km^2, which also has the smallest number of quadrats, occasionally give non-significant results. For road density, one of four replicates is non-significant and for park area, three of four replicates are non-significant.

Table 8. Sample results from an analysis of covariance examining the dependence of NDVI (normalized difference vegetation index) and of TIR (thermal infrared radiation) on natural characteristics of the environment—temperature, precipitation (precipitation$^{0.2}$), and vegetation (10-class categorical variable)—and anthropogenic variables—road density, extent of natural cover, and park area—for a quadrat size of 18825 km^2. Human activity variables entered singly in these models were never significant. Collinearity among climate and anthropogenic variables occasionally resulted in non-significant p-values for model terms.

i. dependent variable: NDVI, $r^2 = 0.96$

variable	S.S.[a]	df[b]	F-ratio	p
(precipitation)$^{0.2}$	6.72×10^4	1	49.17	$<10^{-5}$
temperature	6.63×10^4	1	48.54	$<10^{-5}$
temperature*(precipitation)$^{0.2}$	6.77×10^4	1	49.57	$<10^{-5}$
vegetation	2.56×10^4	8	2.34	0.029
vegetation*road density	4.09×10^3	6	0.50	0.810
vegetation*natural cover	4.85×10^4	7	5.07	$<10^{-3}$
vegetation*park area	3.22×10^4	7	3.37	0.004
error	8.47×10^4			

ii. dependent variable: TIR, $r^2 = 0.98$

variable	S.S.	df	F-ratio	p
(precipitation)$^{0.2}$	7.59×10^2	1	2.75	0.103
temperature	1.37×10^3	1	4.96	0.030
temperature*(precipitation)$^{0.2}$	8.07×10^2	1	2.92	0.093
vegetation	1.74×10^3	7	0.90	0.513
vegetation*road density	1.16×10^3	7	0.60	0.753
vegetation*natural cover	4.62×10^3	8	2.09	0.050
vegetation*park area	1.89×10^3	6	1.14	0.349
error	1.71×10^4	62		

S.S.[a]: sums of squares; df[b]: degrees of freedom

Table 9. Summary of linear regressions (pooled over replicates at each quadrat size) examining the direction of the vegetation-specific responses of NDVI (normalized difference vegetation index) and TIR (thermal infrared radiation) to human activity – road density and extent of natural cover – and protected area status (park area). Results are based on a 10-class vegetation classification. Numerical values indicate how frequently a significant relationship ($p<0.05$) is observed across spatial scales (out of five quadrat sizes) and direction of relationships is indicated by a (+) or (–) sign. Vegetation types are described in more detail in Table 1.

	dependent variable: NDVI			dependent variable: TIR		
vegetation type	road density	natural cover	park area	road density	natural cover	park area
grassland/rangeland (W)	4 +	3 +	2 +	4 –	3 –	1 –
pasture (W)	3 +	3 +	2 +	4 –	4 –	2 –, 1 +
grain/canola (W)	4 –	5 +	5 +	2 +	5 –	5 –
low density pasture (W)	2 –	2 +	3 +	2 +	2 –	3 –
corn/soybean	3 –	1 +	2 +	4 +	1 +	3 –
woodland-agriculture (W)	5 –	4 +	4 +	5 +	5 –	4 –
pasture/forest/cropland (E)	5 –	5 +	5 +	2 +	1 –	ns
low density conifer. forest	2 –, 1 +	2 +	5 –	5 +	3 –, 1 +	1 –, 1 +
conifer. forest w/ broadleaf	3 –	3 +	5 –	5 +	1 –, 2 +	2 –
mixed/open decid. forest	5 –	5 +	4 +	ns	4 +	3 –

Figure 1. Land use map of Canada derived from 1998 SPOT-4/VGT imagery.

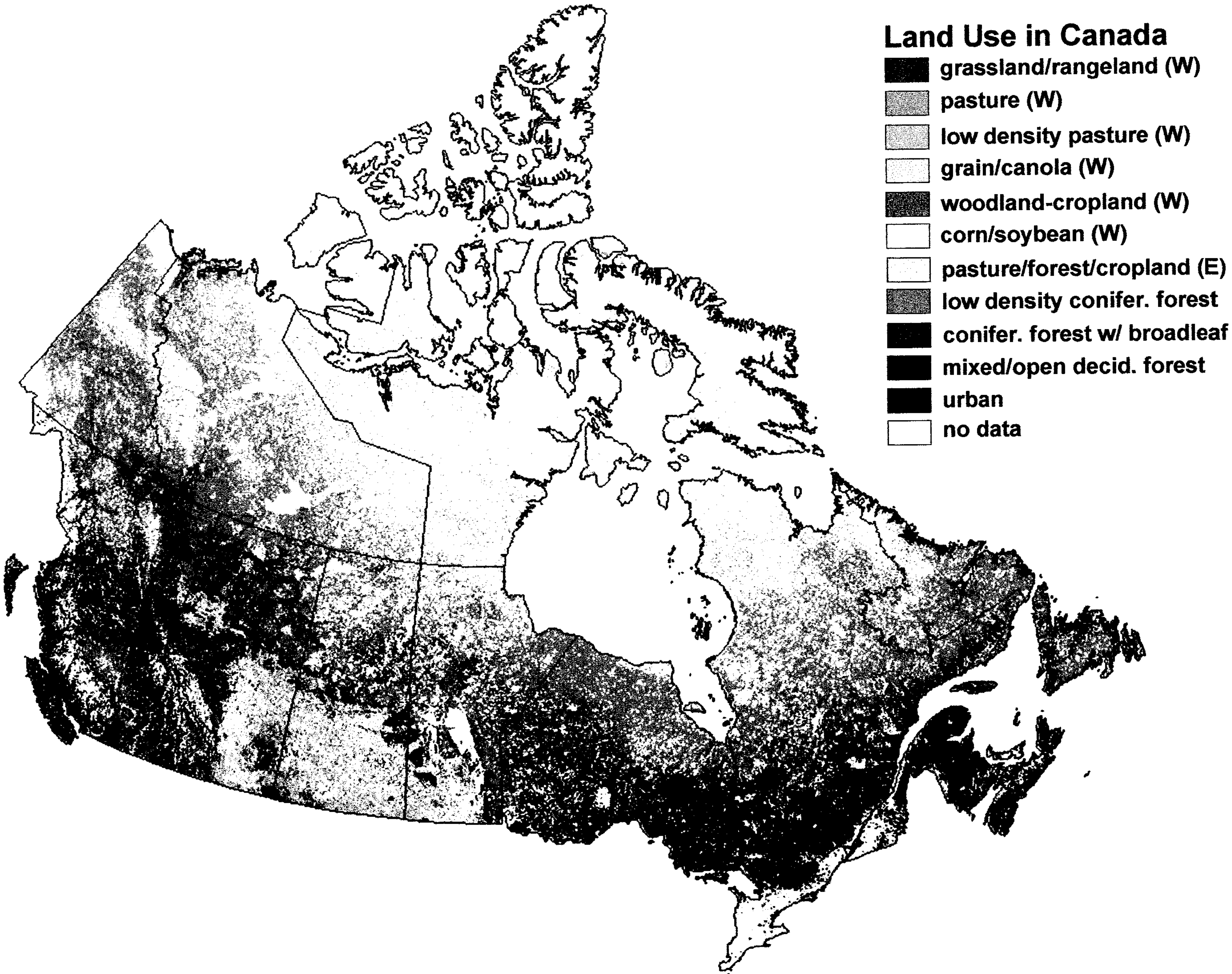
Land Use in Canada
grassland/rangeland (W)
pasture (W)
low density pasture (W)
grain/canola (W)
woodland-cropland (W)
corn/soybean (W)
pasture/forest/cropland (E)
low density conifer. forest
conifer. forest w/ broadleaf
mixed/open decid. forest
urban
no data

Figure 2. Seasonally-averaged normalized difference vegetation index (NDVI) in Canada (1994-2000) for a quadrat size of 675 km^2. NDVI is derived from the visible and near infrared channels of the NOAA-AVHRR sensor.

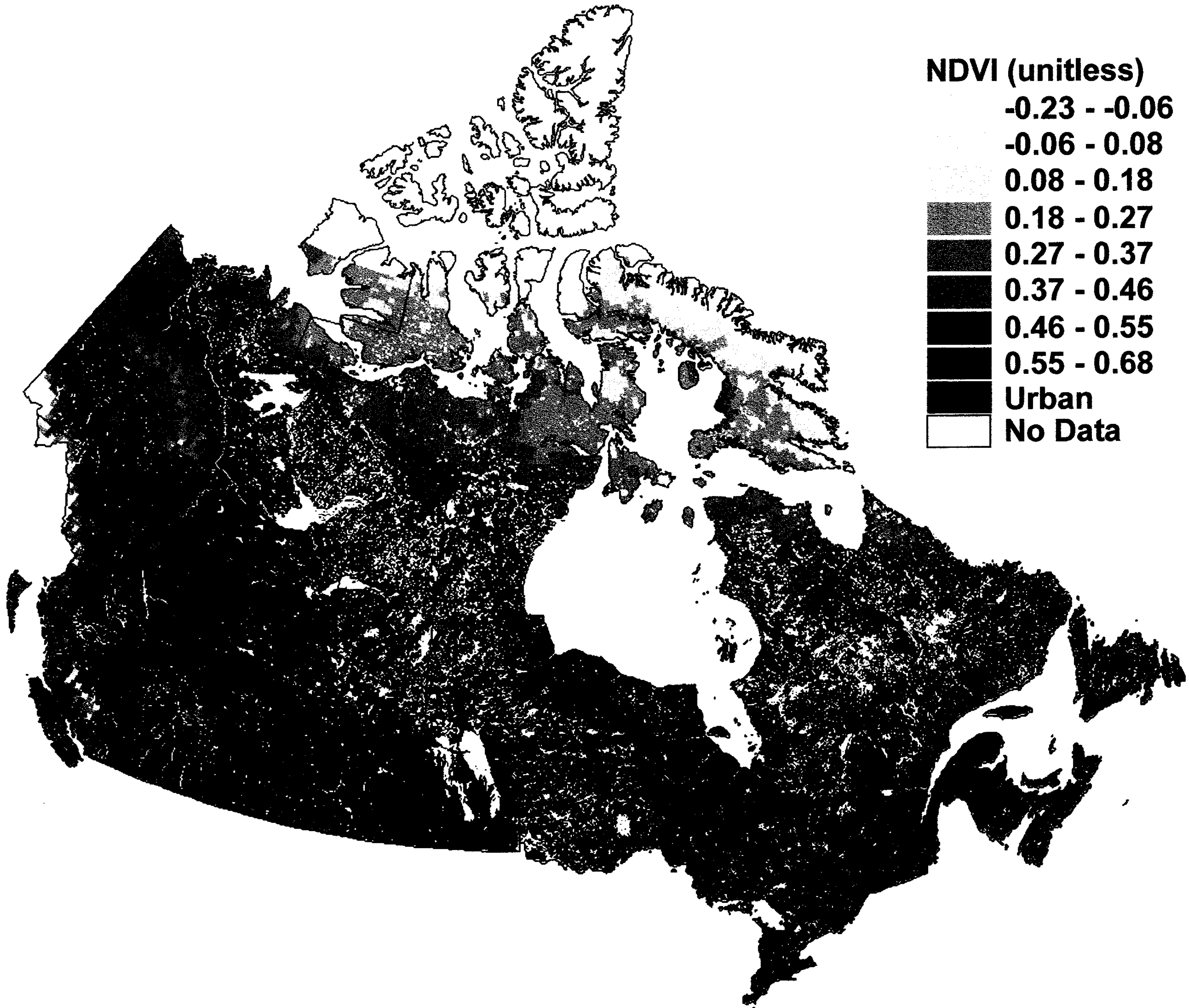
NDVI (unitless)
-0.23 - -0.06
-0.06 - 0.08
0.08 - 0.18
0.18 - 0.27
0.27 - 0.37
0.37 - 0.46
0.46 - 0.55
0.55 - 0.68
Urban
No Data

Figure 3. Seasonally-integrated thermal infrared radiation (TIR) in Canada (1994-2000) for a quadrat size of 675 km^2. TIR is derived from thermal channels 4 and 5 of the NOAA-AVHRR sensor. Sites where TIR is visibly higher than the surrounding landscape include the Okanagan Valley of British Columbia (1); small patches of agriculture in areas of boreal forest north of Lake Huron (2), southern Ontario and the Eastern Townships of Québec (3); and the James Bay-LaGrande hydroelectric project (4).

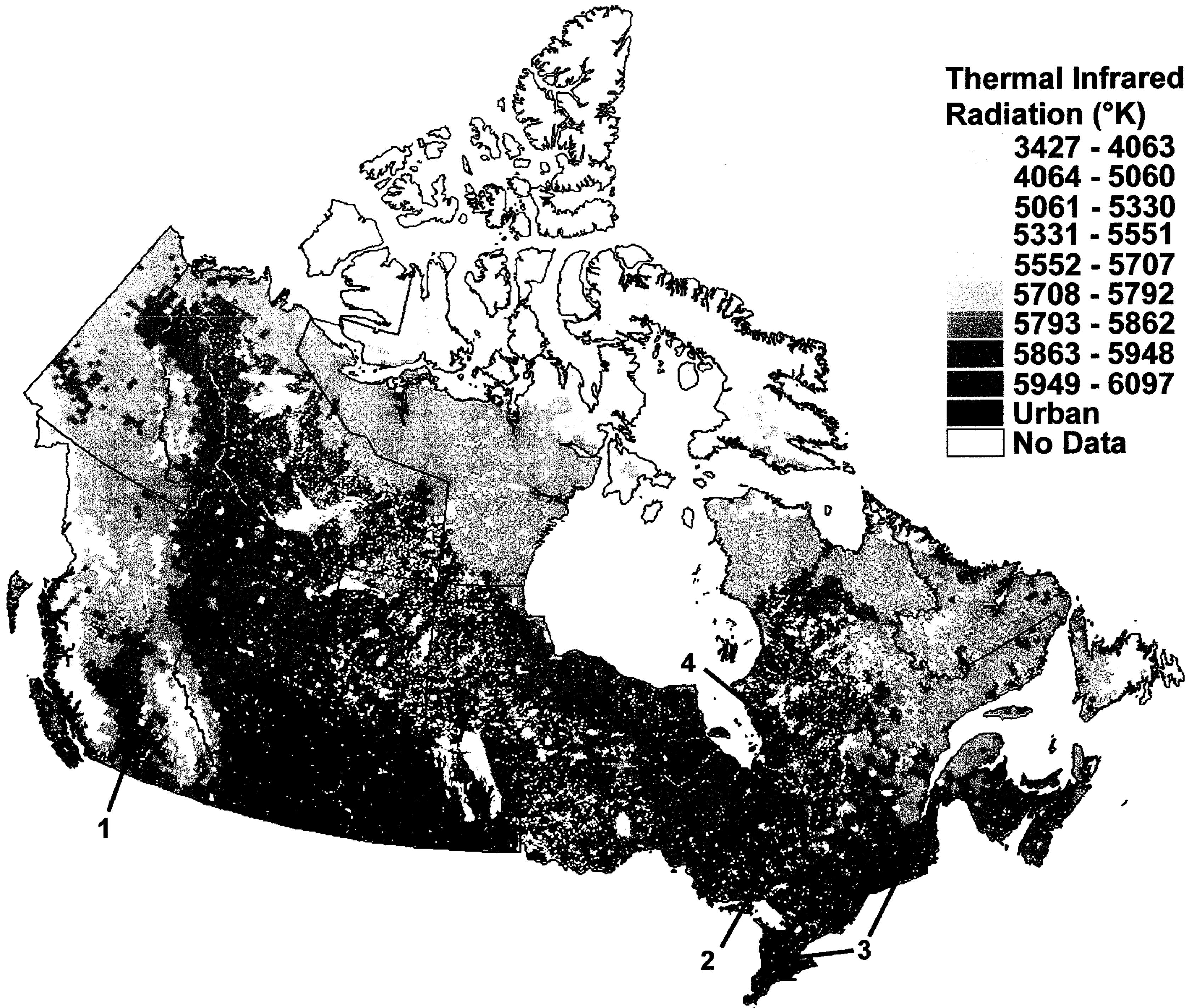
Thermal Infrared
Radiation (°K)
3427 - 4063
4064 - 5060
5061 - 5330
5331 - 5551
5552 - 5707
5708 - 5792
5793 - 5862
5863 - 5948
5949 - 6097
Urban
No Data
1
2
3
4

Figure 4. Total growing season precipitation (April to October) normalized for the years 1961-1990 for a quadrat size of 675 km^2.

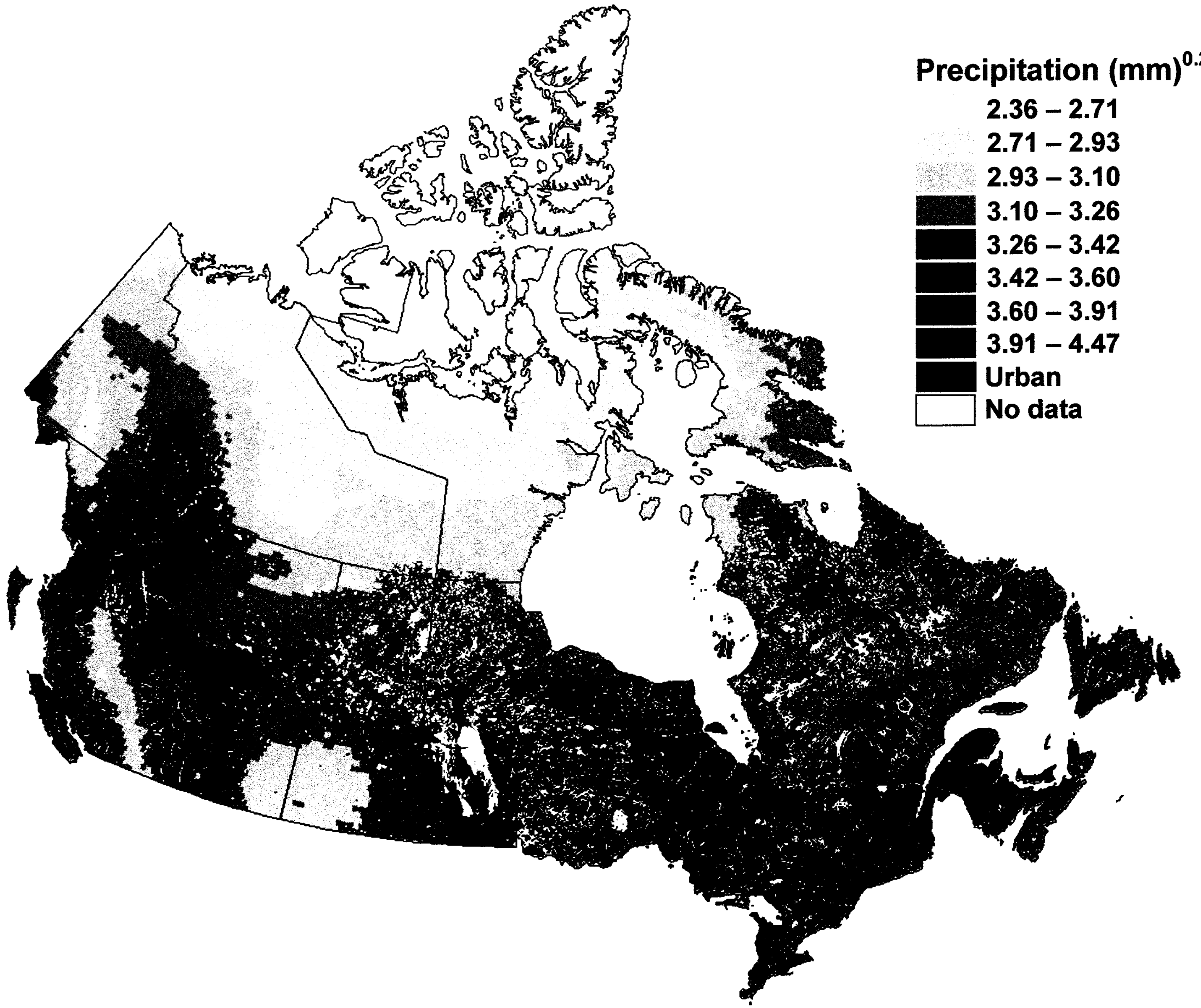

Precipitation (mm)$^{0.2}$
2.36 – 2.71
2.71 – 2.93
2.93 – 3.10
3.10 – 3.26
3.26 – 3.42
3.42 – 3.60
3.60 – 3.91
3.91 – 4.47
Urban
No data

Figure 5. Mean growing season temperature (April to October) normalized for the years 1961 to 1990 for a quadrat size of 675 km^2.

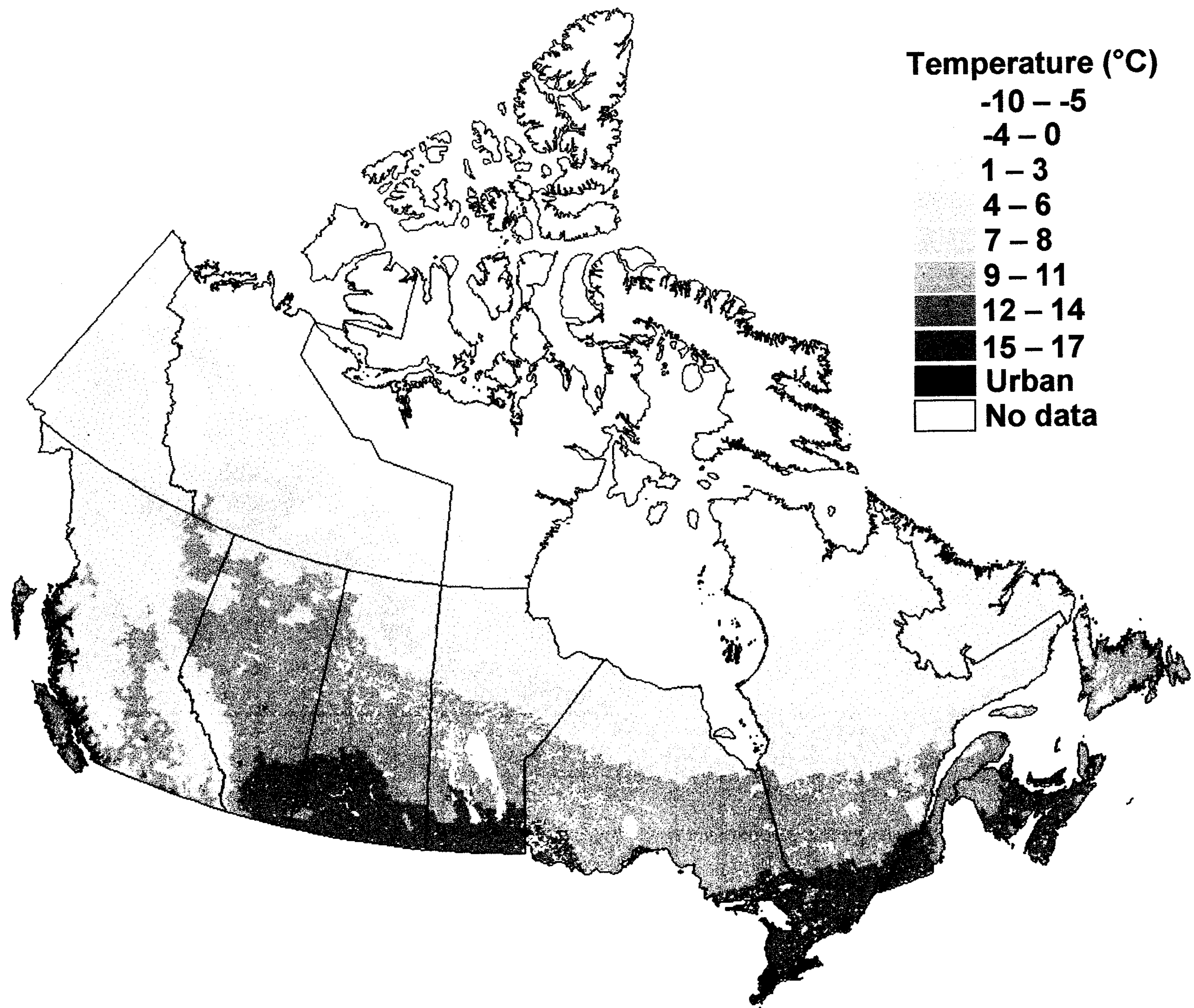
Temperature (°C)
-10 – -5
-4 – 0
1 – 3
4 – 6
7 – 8
9 – 11
12 – 14
15 – 17
Urban
No data

Figure 6. Road density in Canada for a quadrat size of 675 km^2.

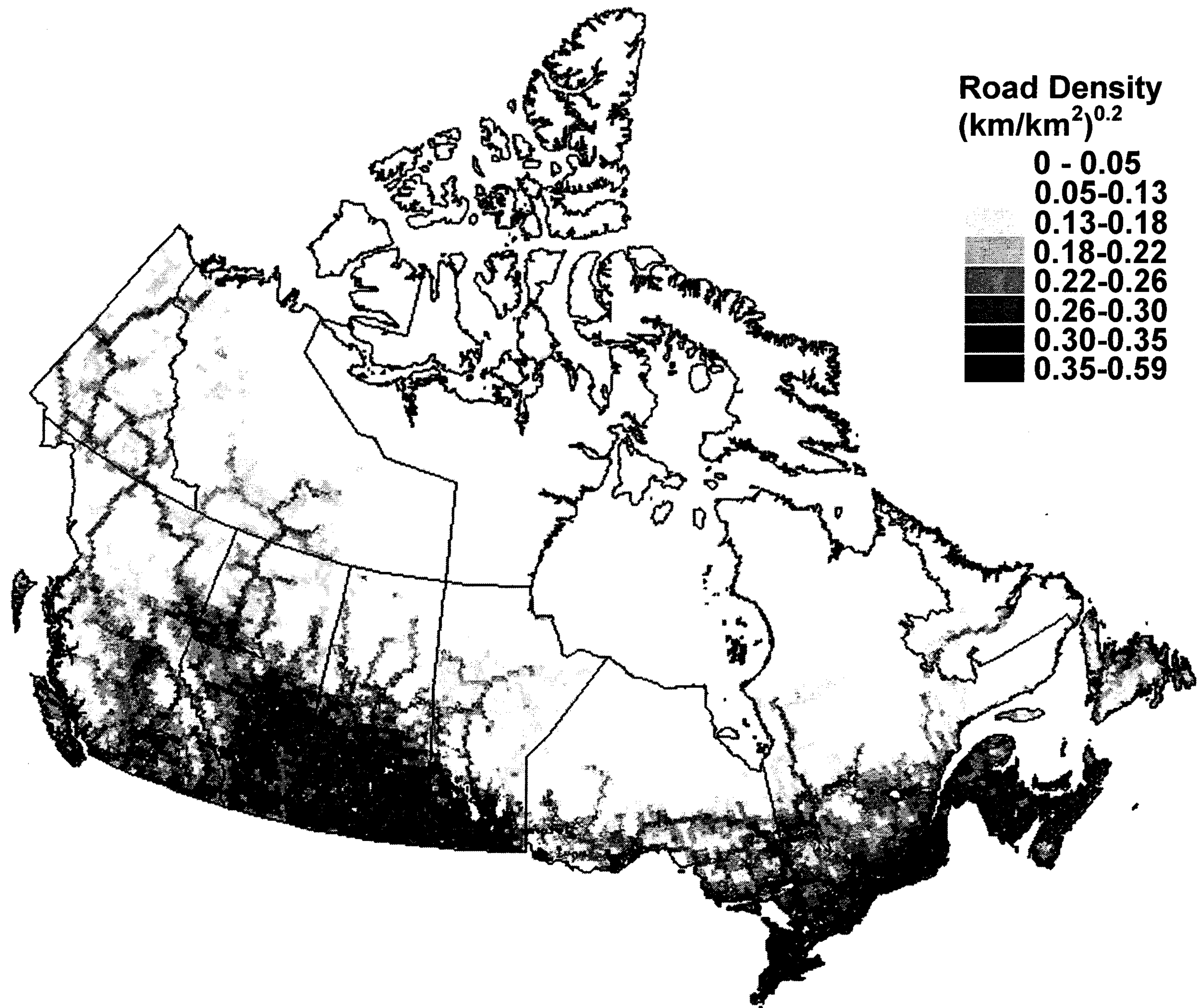
Road Density
(km/km2)0.2
0 - 0.05
0.05-0.13
0.13-0.18
0.18-0.22
0.22-0.26
0.26-0.30
0.30-0.35
0.35-0.59

Figure 7. Protected area status in Canada for a quadrat size of 676 km^2. Protected areas include all national, provincial, and municipal parks and conservation areas.

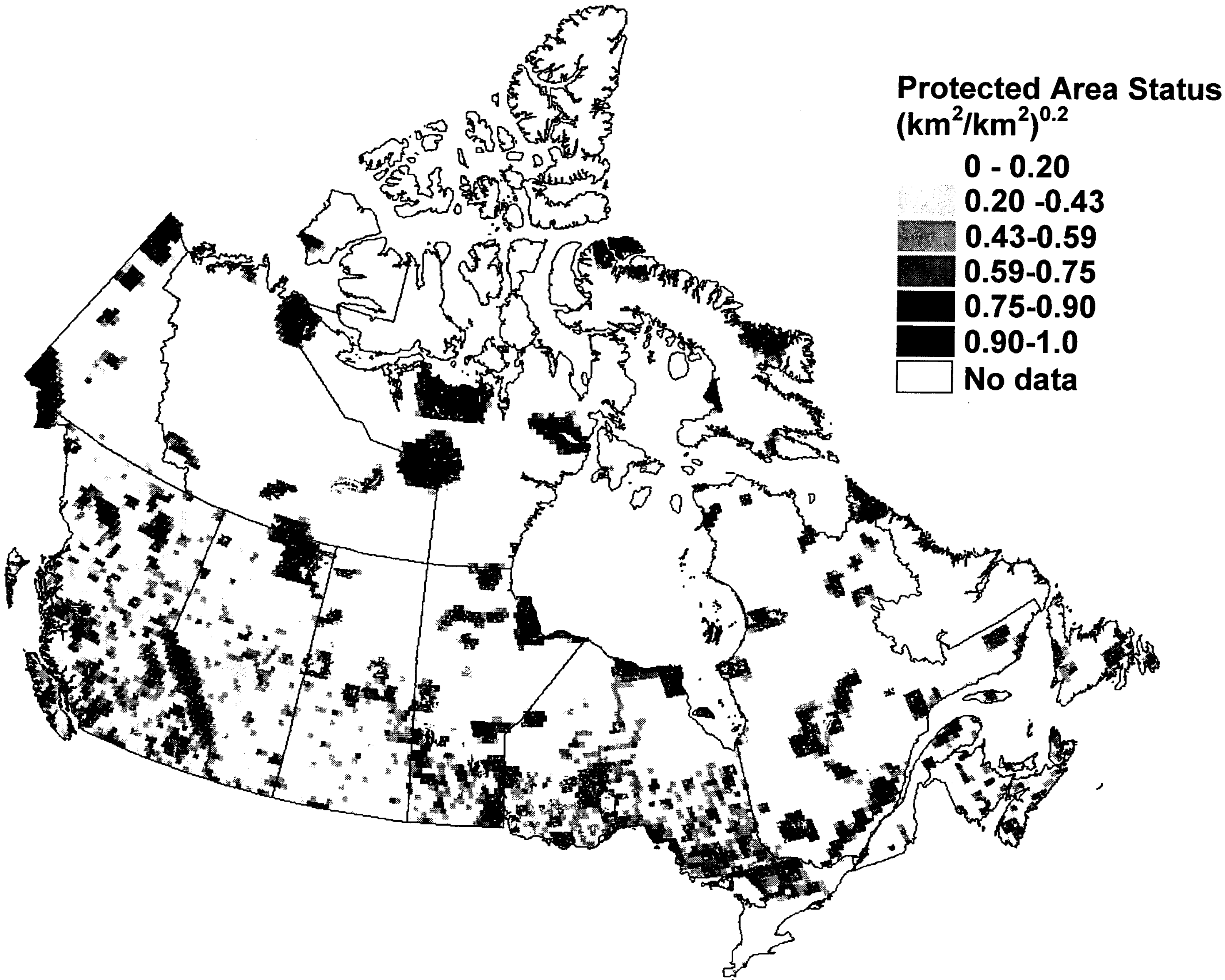
Protected Area Status
(km2/km2)0.2
0 - 0.20
0.20 -0.43
0.43-0.59
0.59-0.75
0.75-0.90
0.90-1.0
No data

Figure 8. Normalized difference vegetation index (NDVI) and thermal infrared radiation (TIR) plotted as a function of human activity (road density, extent of natural cover) and protected area status before controlling for climate and vegetation type, shown for a quadrat size of 18225 km^2. NDVI- and TIR-road density curves are fitted with two separate lines for two different groups of vegetation types: (i) pasture, low density pasture, woodland-agriculture, pasture/forest/cropland, and forest classes (○) and (ii) grassland/pasture, rangeland, and grain/canola (×).

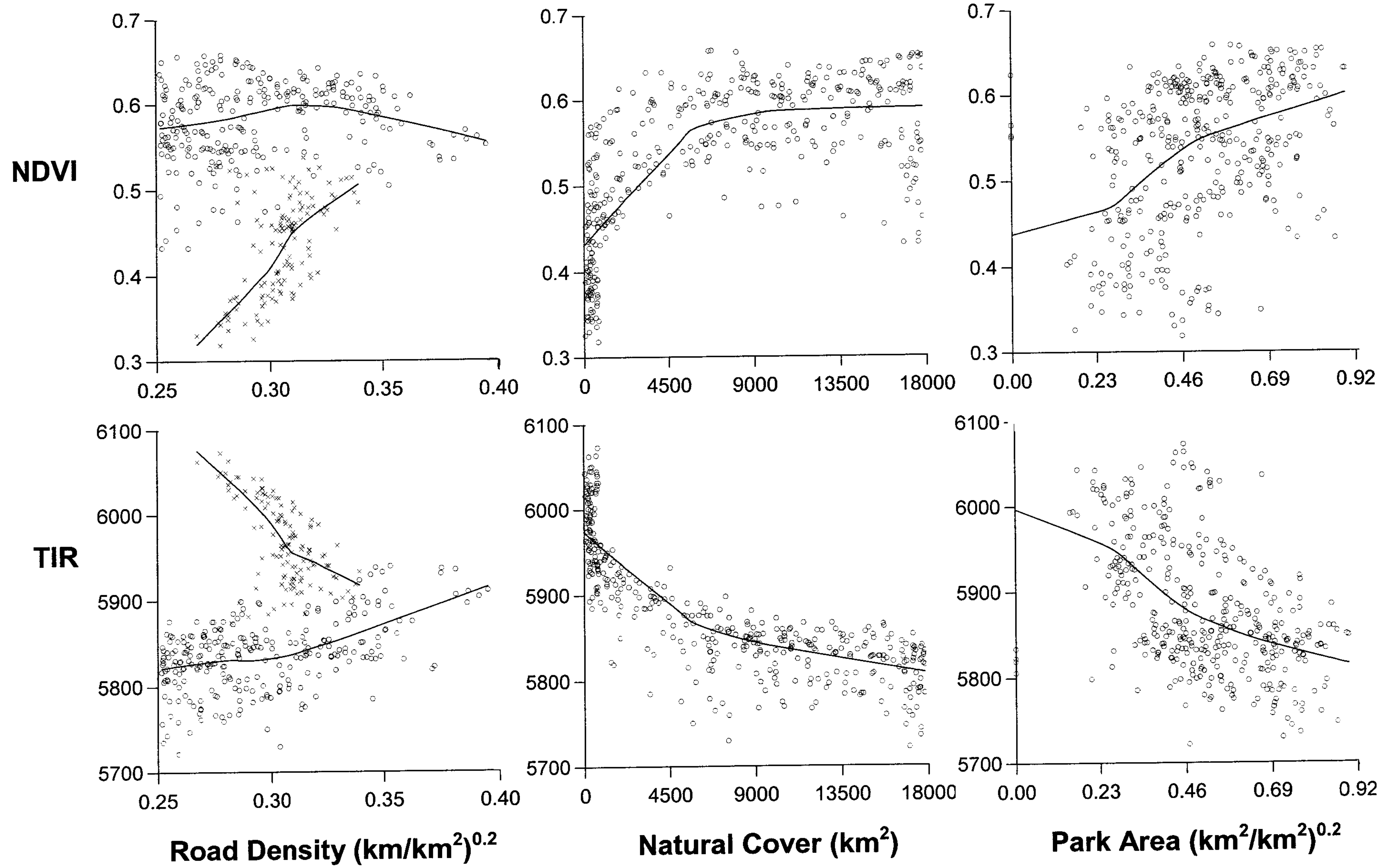
NDVI
TIR
0.7
0.6
0.5
0.4
0.3
6100
6000
5900
5800
5700
0.25
0.30
0.35
0.40
0
4500
9000
13500
18000
0.00
0.23
0.46
0.69
0.92
Road Density (km/km²)^0.2
Natural Cover (km²)
Park Area (km²/km²)^0.2

Figure 9. Normalized difference vegetation index (NDVI) and thermal infrared radiation (TIR) residuals plotted as a function of human activity (road density, extent of natural cover) and protected area status residuals, after controlling for the variation related to climate and vegetation type in both the dependent and independent variables. Relationships are fitted with a Lowess curve and significance is based on linear regressions using data from all four replicates at a quadrat size of 18225 km^2, where each symbol represents a different replicate. All slopes are statistically significant ($p<0.05$).

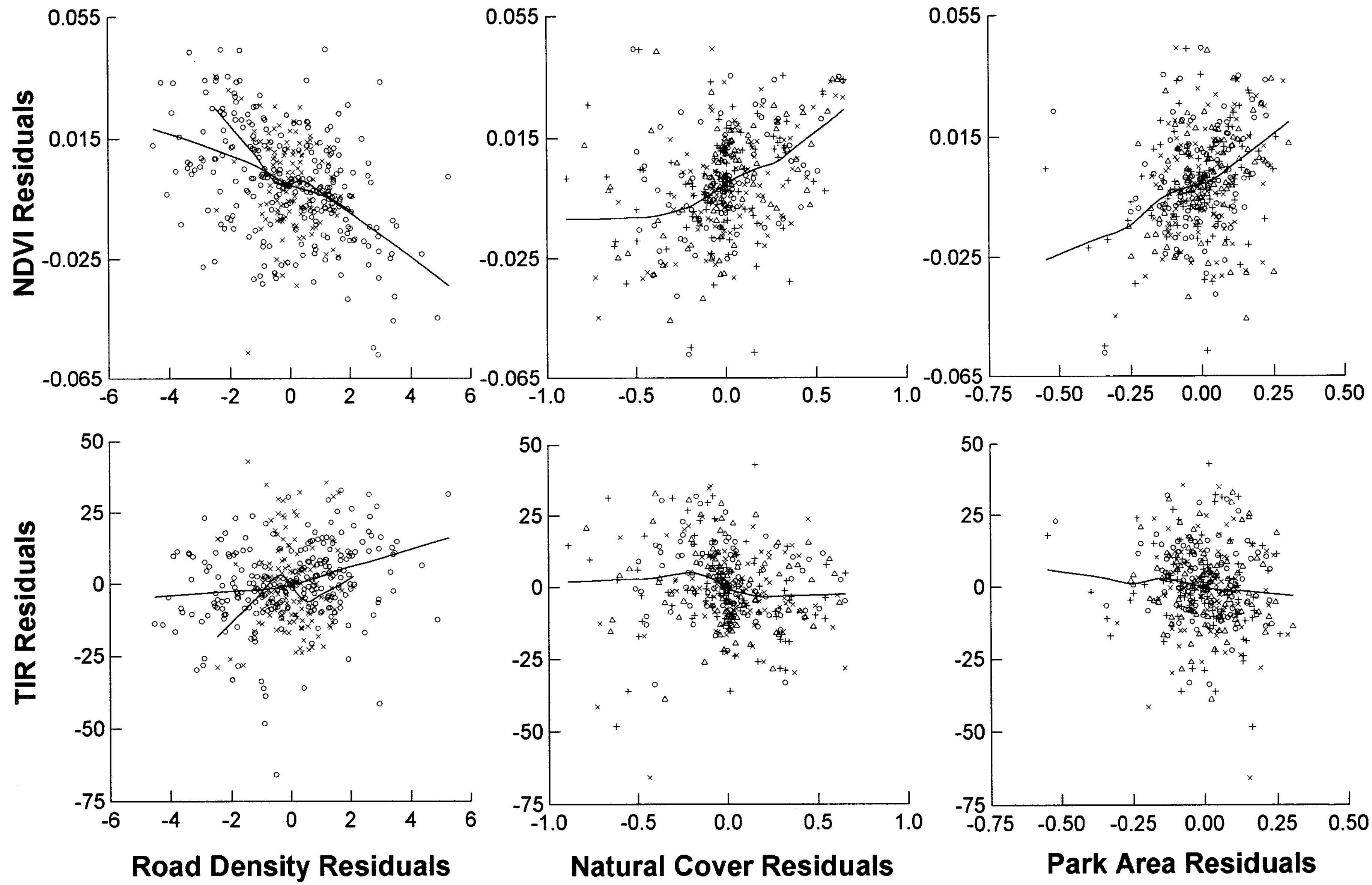
NDVI Residuals
TIR Residuals
Road Density Residuals
Natural Cover Residuals
Park Area Residuals
0.055
0.015
-0.025
-0.065
50
25
0
-25
-50
-75
-6
-4
-2
0
2
4
6
-1.0
-0.5
0.0
0.5
1.0
-0.75
-0.50
-0.25
0.00
0.25
0.50

Figure 10. Above expected and below expected ecosystem function as measured by seasonally-averaged NDVI (normalized difference vegetation index) for a quadrat size of 675 km^2, expressed in units of standard deviation (s.d.). Orange and yellow areas represent ecosystems in which observed NDVI is lower than expected, while green regions are those ecosystems in which NDVI is greater than expected. Grey regions are within one standard deviation of the expected NDVI. Excluded data represent areas with road density less than 0.001 km/km^2.

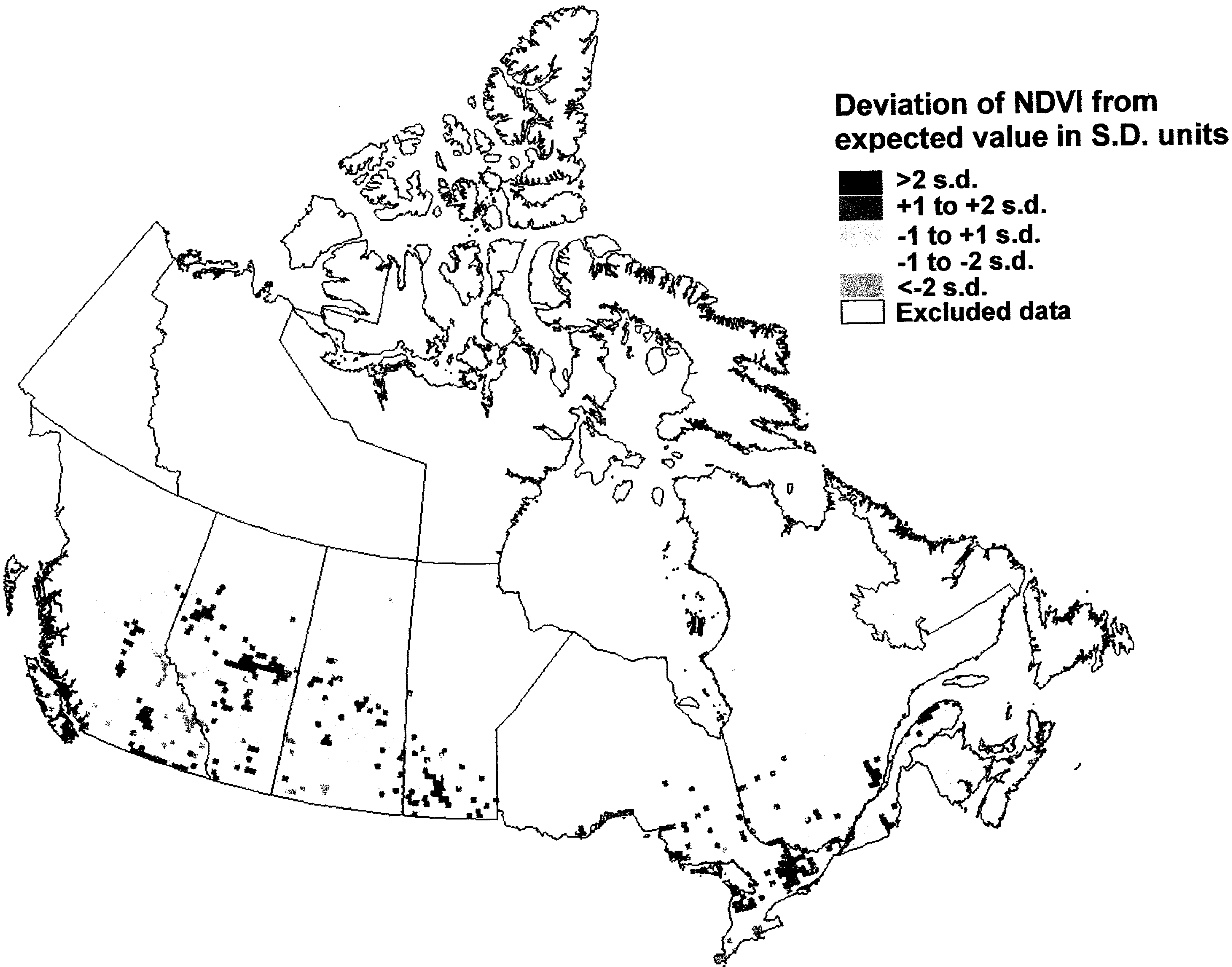
Deviation of NDVI from
expected value in S.D. units
>2 s.d.
+1 to +2 s.d.
-1 to +1 s.d.
-1 to -2 s.d.
<-2 s.d.
Excluded data

Figure 11. Schematic diagram showing the extent to which anthropogenic variables (road density, natural cover, and protected area status) covary with the natural environmental gradient, based on the results of general linear models (Table 6). The size of each bar (drawn to scale) shows the proportion of variation in NDVI (normalized difference vegetation index) statistically explained by the total model (natural + human), natural only, human only, and natural or human. Variance was partitioned by examining the amounts of variance statistically explained when variables were added sequentially into regression models.

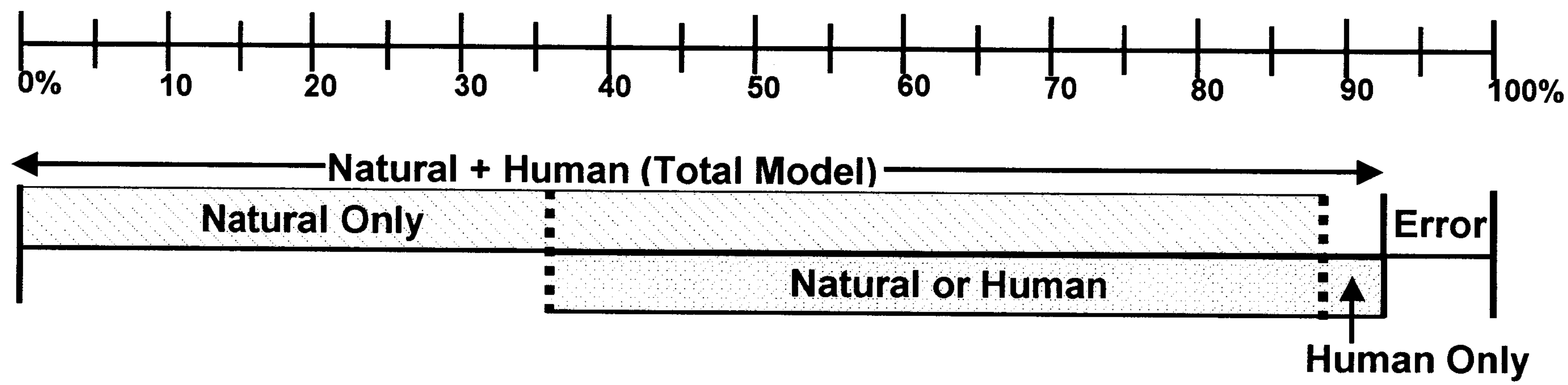
0%
10
20
30
40
50
60
70
80
90
100%
Natural + Human (Total Model)
Natural Only
Natural or Human
Error
Human Only

Appendix A. The mean, range, and standard deviation (s.d.) among quadrats, by vegetation type, of the ecosystem function, climate, and human activity variables used in this study for a quadrat size of 225 km^2 (finest spatial scale).

variable	vegetation type	mean	range	s.d.
NDVI	grassland/rangeland	0.32	0.27 – 0.40	0.02
(seasonally integrated	pasture	0.44	0.32 – 0.57	0.06
normalized difference	grain/canola	0.44	0.30 – 0.57	0.05
vegetation index)	low density pasture	0.51	0.42 – 0.58	0.04
(unitless)	woodland-agriculture	0.53	0.43 – 0.64	0.03
	corn/soybean	0.54	0.42 – 0.62	0.03
	pasture/forest/cropland	0.58	0.42 – 0.66	0.04
	low density conifer. forest	0.52	0.28 – 0.61	0.05
	conifer. forest w/ broadleaf	0.58	0.35 – 0.70	0.05
	mixed/open decid. forest	0.62	0.39 – 0.68	0.03
TIR (seasonally	grassland/rangeland	6064.	6001. – 6103.	21.
integrated thermal	pasture	5981.	5847. – 6089.	54.
infrared radiation)	grain/canola	5960.	5830. – 6072.	42.
(°K)	low density pasture	5920.	5810. – 6001.	50.
	woodland-agriculture	5889.	5787. – 5994.	30.
	corn/soybean	5913.	5823. – 5980.	27.
	pasture/forest/cropland	5876.	5734. – 5980.	39.
	low density conifer. forest	5835.	5578. – 6009.	50.
	conifer. forest w/ broadleaf	5807.	5620. – 5953.	36.
	mixed/open decid. forest	5825.	5608. – 5920.	34.
$(\text{precipitation})^{0.2}$	grassland/rangeland	3.01	2.94 – 3.10	0.03
(mm)	pasture	3.15	2.95 – 3.46	0.10
	grain/canola	3.16	2.90 – 3.66	0.09
	low density pasture	3.21	2.98 – 3.43	0.08
	woodland-agriculture	3.26	3.08 – 3.84	0.09
	corn/soybean	3.57	3.28 – 3.77	0.06
	pasture/forest/cropland	3.59	3.45 – 3.81	0.09
	low density conifer. forest	3.29	2.87 – 3.81	0.19
	conifer. forest w/ broadleaf	3.47	2.90 – 4.28	0.23
	mixed/open decid. forest	3.58	3.03 – 4.20	0.16

Appendix A. continued

variable	vegetation type	mean	range	s.d.
temperature (°C)	grassland/rangeland	12.5	10.9 – 13.4	0.5
	pasture	11.6	8.6 – 13.4	1.0
	grain/canola	11.6	9.0 – 13.7	0.8
	low density pasture	11.1	8.9 – 12.8	1.0
	woodland-agriculture	10.7	8.1 – 13.9	1.0
	corn/soybean	14.0	9.3 – 16.5	1.1
	pasture/forest/cropland	13.1	9.6 – 16.7	1.3
	low density conifer. forest	9.0	3.3 – 14.5	1.9
	conifer. forest w/ broadleaf	9.5	3.6 – 13.7	1.6
	mixed/open decid. forest	11.0	5.2 – 16.1	1.2
(road density)$^{0.2}$ (km/km^2)	grassland/rangeland	0.278	0.251 – 0.340	0.018
	pasture	0.297	0.251 – 0.401	0.023
	grain/canola	0.311	0.251 – 0.474	0.024
	low density pasture	0.297	0.251 – 0.394	0.023
	woodland-agriculture	0.299	0.252 – 0.479	0.028
	corn/soybean	0.345	0.276 – 0.499	0.040
	pasture/forest/cropland	0.350	0.252 – 0.523	0.044
	low density conifer. forest	0.281	0.251 – 0.501	0.028
	conifer. forest w/ broadleaf	0.284	0.251 – 0.426	0.027
	mixed/open decid. forest	0.298	0.251 – 0.505	0.032
natural cover (km^2)	grassland/rangeland	8.	0. – 58.	12.
	pasture	7.	0. – 106.	13.
	grain/canola	8.	0. – 143.	13.
	low density pasture	33.	0. – 133.	29.
	woodland-agriculture	32.	0. – 151.	29.
	corn/soybean	7.	0. – 90.	11.
	pasture/forest/cropland	36.	0. – 134.	29.
	low density conifer. forest	192.	21. – 231.	39.
	conifer. forest w/ broadleaf	200.	45. – 234.	37.
	mixed/open decid. forest	184.	22. – 238.	50.
(park area)$^{0.2}$ (km^2/km^2)	grassland/rangeland	0.07	0. – 0.92	0.20
	pasture	0.10	0. – 0.92	0.21
	grain/canola	0.06	0. – 0.81	0.17
	low density pasture	0.17	0. – 0.83	0.26
	woodland-agriculture	0.25	0. – 1.00	0.31
	corn/soybean	0.03	0. – 0.66	0.10
	pasture/forest/cropland	0.06	0. – 0.90	0.16
	low density conifer. forest	0.20	0. – 1.00	0.33
	conifer. forest w/ broadleaf	0.25	0. – 1.00	0.34
	mixed/open decid. forest	0.22	0. – 1.00	0.33

Appendix B. Normalized difference vegetation index (NDVI) and thermal infrared radiation (TIR) residuals plotted as a function of road density residuals after controlling for the variation related to climate in both the dependent and independent variables. Mixed/open deciduous forest and woodland-cropland are representative of the general relationship observed within vegetation types. Linear regressions were used to determine the direction of the slope in each vegetation type at each quadrat size.

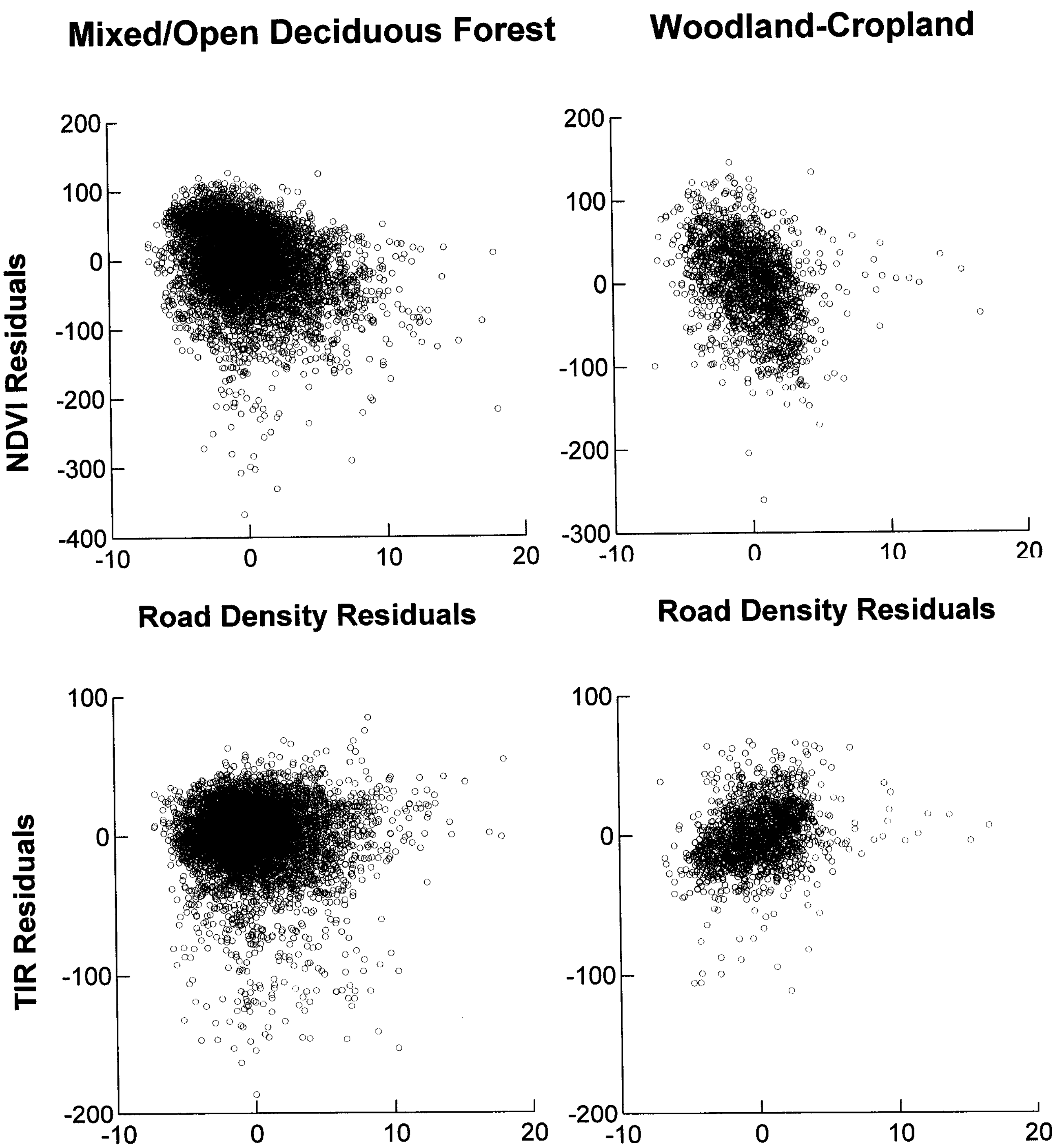

Quadrat size: 225 km^2

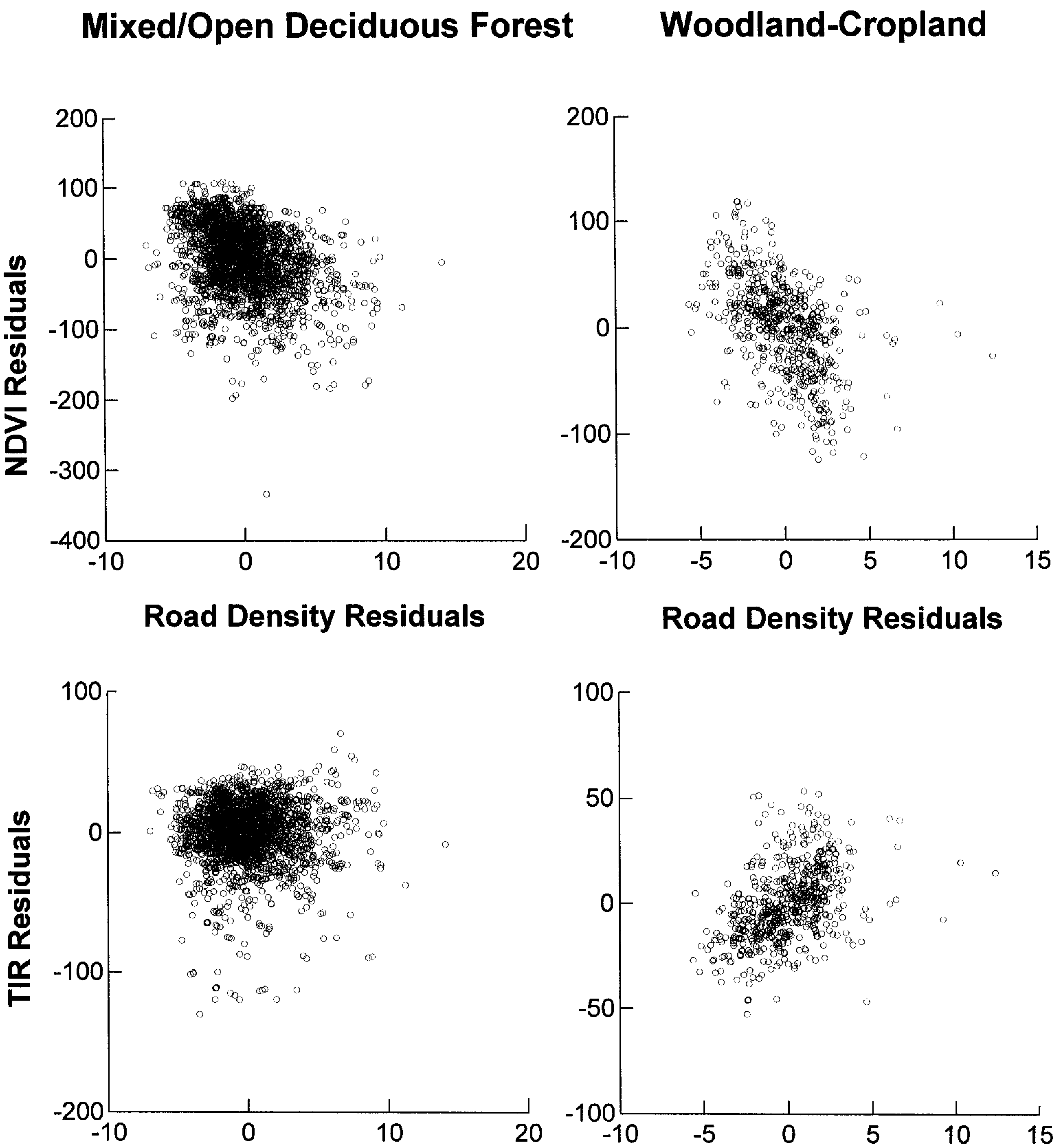

Quadrat size: 675 km^2

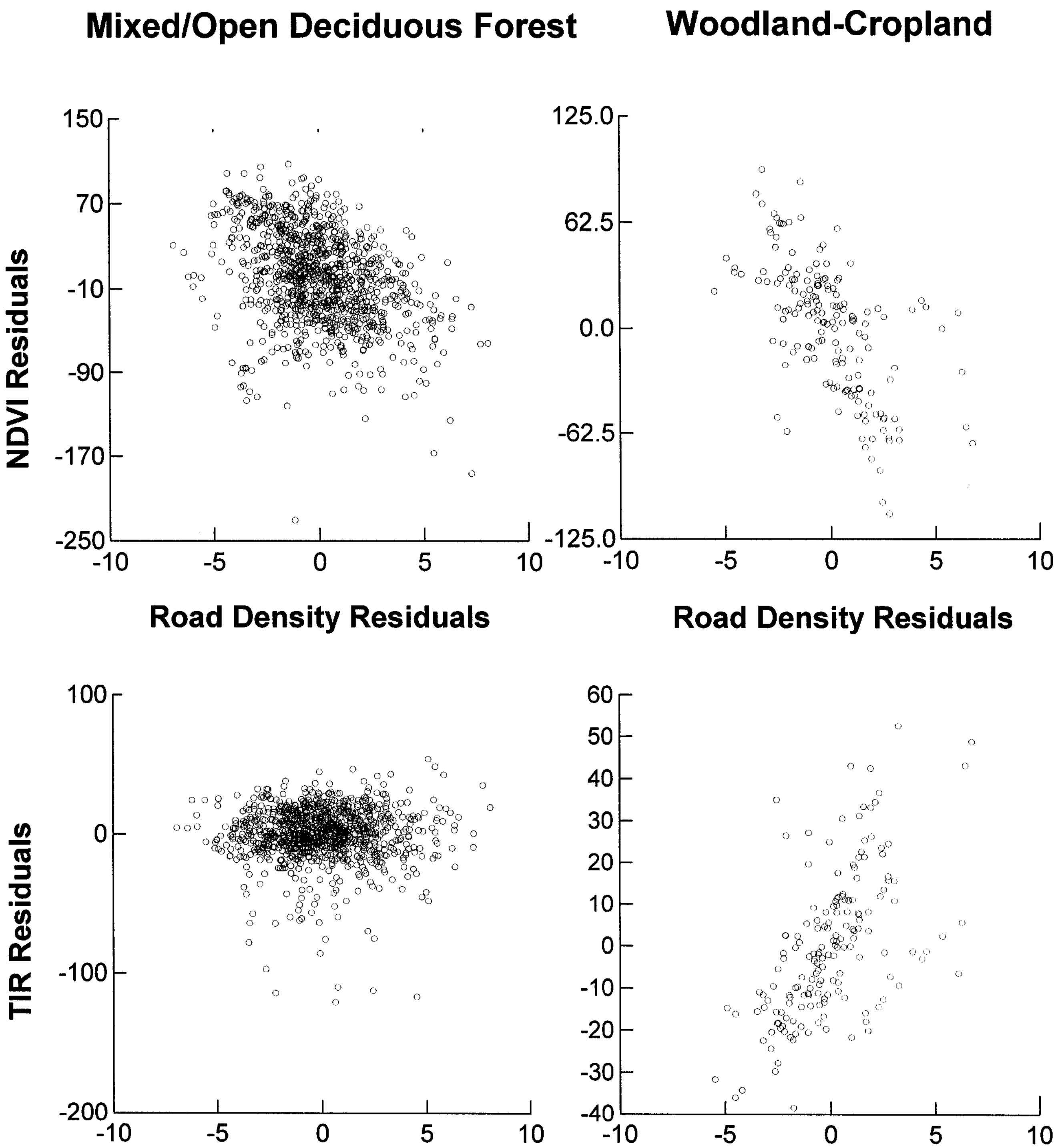

Quadrat size: 2025 km^2

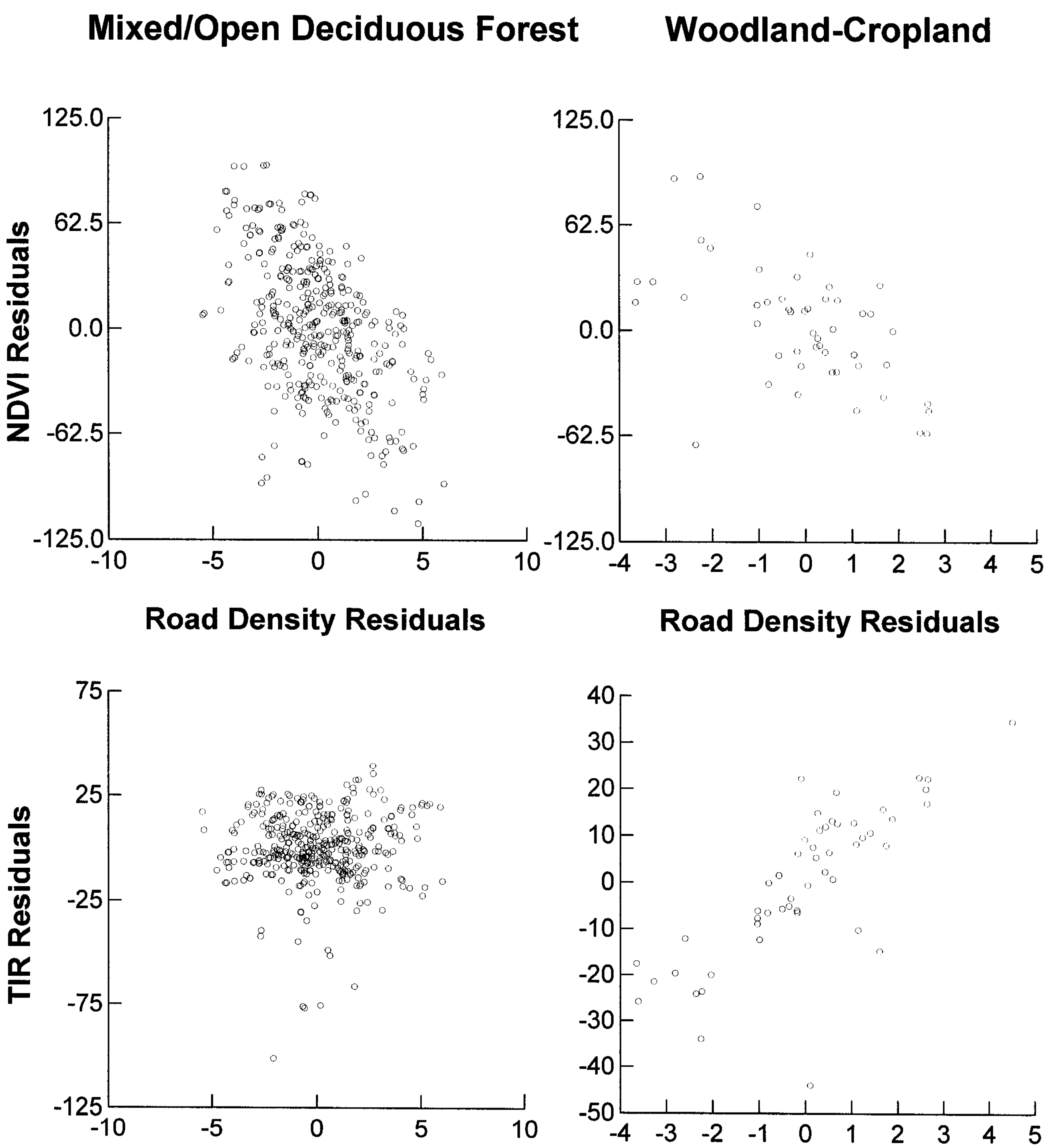

Quadrat size: 6075 km^2

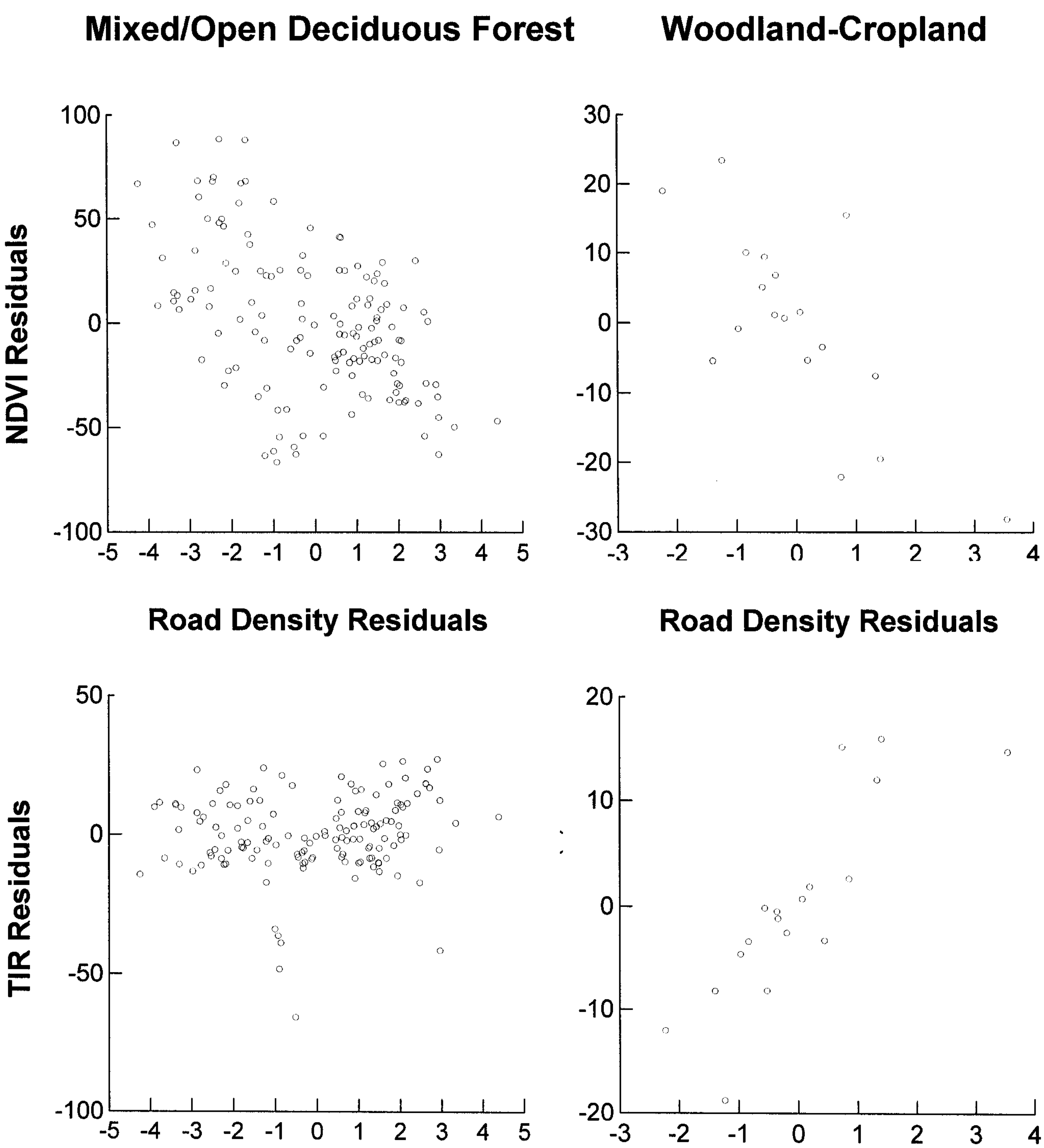

Quadrat size: 18225 km^2